AFRL-MN-EG-TR-2001-7082

AEROBALLISTIC RANGE TESTS OF MISSILE CONFIGURATIONS WITH NON-CIRCULAR CROSS SECTIONS

Wayne H. Hathaway
Arrow Tech Associates
1233 Shelburne Road, Suite D-8
South Burlington, Vermont 05403

Captain Benjamin Kruggel
Gregg Abate
Gerald Winchenbach
John Krieger
AFRL/MNAV
Eglin AFB, Florida 32542

CONTRACT NUMBER F08630-96-C-0001

September 2001

FINAL REPORT FOR PERIOD JANUARY 2000 to DECEMBER 2000

DISTRIBUTION A: Approved for public release; distribution unlimited.

AIR FORCE RESEARCH LABORATORY, MUNITIONS DIRECTORATE
Air Force Material Command ■ United States Air Force ■ Eglin Air Force Base

NOTICE

When Government drawings, specifications, or other data are used for any purpose other than in connection with a definitely Government-related procurement, the United States Government incurs no responsibility or any obligation whatsoever. The fact that the Government may have formulated or in any way supplied the said drawings, specifications, or other data, is not to be regarded by implication, or otherwise in any manner construed, as licensing the holder, or any other person or corporation; or as conveying any rights or permission to manufacture, use, or sell any patented invention that may in any way be related thereto.

This technical report is releasable to the National Technical Information Services (NTIS). At NTIS it will be available to the general public, including foreign nations.

Contract Number: F08630-96-C-0001

Contractor: Arrow Tech Associates
1233 Shelburne Rd. Ste. D-8
S. Burlington, VT 05403

This technical report has been reviewed and is approved for publication.

FREDERICK A. DAVIS
Technical Director
Assessment and Demonstrations Division

GREGG ABATE
Program Manager
Flight Vehicles Integration Branch

Anyone having need for a copy of this report should first contact the Defense Technical Information Center (DTIC) at the address shown below. If you are a registered DTIC User, DTIC can provide you with a copy. Please do not request copies from the Air Force Research Laboratory, Munitions Directorate. Requests for additional copies should be directed to:

Defense Technical Information Center (DTIC)
8725 John J. Kingman Road, Ste 0944
Ft Belvoir, VA 22060-6218

This report is published in the interest of the scientific and technical information exchange. Publication of this report does not constitute approval or disapproval of the ideas or findings.

If your address has changed, if you wish to be removed from our mailing list, or if your organization no longer employs the addressee, please notify AFRL/MNAV, 101 W. Eglin Blvd., Suite 332, Eglin AFB FL 32542-6810, to help us maintain a current mailing list.

Do not return copies of this report unless contractual obligations or notice on a specific document requires that it be returned.

REPORT DOCUMENTATION PAGE			*Form Approved OMB No. 0704-0188*
Public reporting burden for this collection of information is estimated to average 1 hour per response, including the time for reviewing instructions, searching existing data sources, gathering and maintaining the data needed, and completing and reviewing the collection of information. Send comments regarding this burden estimate or any other aspect of this collection of information, including suggestions for reducing this burden, to Washington Headquarters Services, Directorate for Information Operations and Reports, 1215 Jefferson Davis Highway, Suite 1204, Arlington, VA 22202-4302, and to the Office of Management and Budget, Paperwork Reduction Project (0704-0188), Washington, DC 20503.			
1. AGENCY USE ONLY *(Leave blank)*	2. REPORT DATE September 2001	3. REPORT TYPE AND DATES COVERED Final Report January 2000 - December 2000	
4. TITLE AND SUBTITLE AEROBALLISTIC RANGE TESTS OF MISSILE CONFIGURATIONS WITH NON-CIRCULAR CROSS SECTIONS			5. FUNDING NUMBERS C: F08630-96-C-0001 PE: 62602F PR: 2502 TA: 67 WU: 01
6. AUTHOR(S) Wayne H Hathaway (Arrow Tech), Captain Benjamin Kruggel (AFRL/MNAV), Gregg Abate (AFRL/MNAV),Gerald Winchenbach (AFRL/MNAV), and John Krieger (AFRL/MNAV)			
7. PERFORMING ORGANIZATION NAME(S) AND ADDRESS(ES) Arrow Tech Associates 1233 Shelburne Road, Suite D-8 South Burlington VT 05403			8. PERFORMING ORGANIZATION REPORT NUMBER
9. SPONSORING/MONITORING AGENCY NAME(S) AND ADDRESS(ES) Air Force Research Laboratory Munitions Directorate Assessment and Demonstrations Division Flight Vehicles Integration Branch (AFRL/MNAV), Eglin AFB FL 32542-6810 Point of Contact: Gregg Abate, 850-882-4085			10. SPONSORING/MONITORING AGENCY REPORT NUMBER AFRL-MN-EG-TR-2001-7082
11. SUPPLEMENTARY NOTES SUBJECT TO EXPORT CONTROL LAWS. Availability of report is specified on front cover			
12a. DISTRIBUTION/AVAILABILITY STATEMENT DISTRIBUTION A: Approved for public release; distribution unlimited			12b. DISTRIBUTION CODE
13. ABSTRACT *(Maximum 200 words)* Non-axisymmetric body shapes are currently being considered by weapon designers. These applications and requirements include increased range, increased maneuverability, and conformal stores to reduce aircraft drag or radar signature. The objective of this test program is to obtain experimental aerodynamics on several basic cross sectional shape variations. The resulting database will serve to supplement the existing database of experimentally determined aerodynamics and will be used to improve current analytical methodologies associated with aerodynamic predictions. Aerodynamic force and moment coefficients have been extracted from the measured free-flight data in the AFRL Aeroballistic Research Facility (ARF). The range of Mach numbers covered during these trials included Mach 0.75 to 3.5 and comprised a total of 104 flights. A total of seven configurations were tested and evaluated at the ARF: four-fin circular, three-fin circular, 0.8 eccentric elliptical (four-fin), 0.6 eccentric elliptical (four-fin), 0.8/0.6 eccentric blended elliptical (four-fin), four-fin square, and three-fin triangular. These experimental test results provide a good comparison of the shape effects on the basic aerodynamics with respect to axial force, normal force, and pitching moment.			
14. SUBJECT TERM Elliptic Bodies, Non-Circular Cross Section, Experimental Aerodynamics, Spark range tests, Trajectory analysis, Aerodynamics			15. NUMBER OF PAGES 86 16. PRICE CODE
17. SECURITY CLASSIFICATION OF REPORT UNCLASSIFIED	18. SECURITY CLASSIFICATION OF THIS PAGE UNCLASSIFIED	19. SECURITY CLASSIFICATION OF ABSTRACT UNCLASSIFIED	20. LIMITATION OF ABSTRACT UL

NSN 7540-01-280-5500

Standard Form 298 (Rev. 2-89)
Prescribed by ANSI Std. 239-18

INTENTIONALLY LEFT BLANK

PREFACE

This report documents the aerodynamic coefficients and stability derivatives resulting from a series of free flight tests of a generic missile configuration with circular and non-circular cross sections over a Mach number range of 0.75 through 3.5. All configurations had a common rectangular tail fin design and were either of a three-fin of four-fin variety depending upon the missile cross-section These tests were conducted in the USAF Aeroballistic Research Facility, located at Eglin AFB, FL. The period of testing covered a time period of 1997 to 2000.

The data analysis was accomplished by the Arrow Tech Associates of South Burlington, Vermont 05401-4985, under Contract F08630-96-C-0001, with the Air Force Research Laboratory Munitions Directorate, Eglin Air Force Base, Florida 32542-5434. Mr. Gerald Winchenbach, Dr. Gregg Abate, and Captain Benjamin Kruggel of AFRL were the principal investigators and test directors. Mr. John Krieger of the ARF conducted the test that included launch, instrumentation, data acquisition, and image processing.

INTENTIONALLY LEFT BLANK

TABLE OF CONTENTS

INTENTIONALLY LEFT BLANK

LIST OF FIGURES

Figure page

LIST OF TABLES

SECTION I

INTRODUCTION

Current munition designs are departing from conventional right circular cross-sections for many reasons including enhanced performance, increased range, increased maneuverability, and stealth. Improved manufacturing and production capability for both metal and composite structures is also leading weapon designers to consider non-circular vehicle shapes. The objective of this effort is to obtain an experimental aerodynamic database on several basic cross sectional shape variations within a free-flight ballistics range. The results will serve to supplement existing data and will be used to improve current analytical design methodologies that estimate vehicle aerodynamics. A total of seven configurations were tested. The models were designed to have an equivalent cross sectional area and identical fin planform to isolate effects due to the body alone. The primary goals for this effort are (1) to determine shape effects on the aerodynamics and (2) provide an experimental database for aeroprediction methodology.

The free-flight ballistic range has several advantages compared to wind tunnels for aerodynamic research. The most important one is that the test object is in unrestrained flight. Thus, no model support (sting) or wall interference effects are present during the measurement of the data. Additionally, the ballistic range allows for the determination of aerodynamic stability coefficients and derivatives that are not easily measured in a wind tunnel. Each trial conducted in the ballistic range results in a unique initial starting attitude (initial conditions) upon launch resulting in pitch and yaw motion that enables the test engineers to determine the dynamic derivatives and coefficients. Analyzing two or more trials simultaneously results in a common set of aerodynamic parameters of the configuration independent of initial conditions. This can be done over a range of Mach numbers to determine the aerodynamic parameters as a function of Mach number. It is also desirable to have trials with sufficient pitch and yaw amplitudes to cover the angle-of-attack regime of interest. A drawback of ballistic range testing is size limitations. Typical free-flight models are sub-scale so matching the full scale Reynolds number if difficult or impossible. However, this is also a limitation of wind tunnel tests and, in either case, care must be used when interrupting results.

One challenge in free flight testing is the model design and construction. Since the model is typically launched via circular tube (e.g., powder gun) it must be encased within a sabot for launch. In addition, the model/sabot package must be sized to fit the particular launcher and be capable of withstanding the in–bore accelerations. Therefore, the size of the model is often small and results in high precision tolerances during manufacture. The in-bore acceleration requirement means that the model/sabot design must capable of surviving the launch cycle. Hence, the models require adequate strength to be launched without suffering structural damage.

This report documents the aerodynamic coefficients and stability derivatives extracted from trajectory data collected during free flight tests of five non-axisymmetric configurations. In addition, two circular configurations were tested to establish a baseline reference for the results. The models were designed so that the cross-sectional area was common for all configurations. The tests were conducted in the USAF Aeroballistic Research Facility. During this period of the tests, the Flight Vehicle Integration Branch of the Air Force Research Laboratory Munitions Directorate solely maintained and operated the Facility. Recently, the University of Florida Graduate Engineering and Research Center (UF/GERC) has become a partner in the management of the facility.

SECTION II

AEROBALLISTIC TESTING

1. Aeroballistic Research Facility

The Aeroballistic Research Facility[1] (ARF) is an enclosed concrete structure used to examine the exterior ballistics of various free-flight configurations. The facility contains a gun room, control room, model measurement room, blast chamber, and an instrumented range. Figure 1 contains an illustration of the ARF and an interior view. The range atmosphere is controlled and closely monitored.

The 200-meter range has a 16-square meter cross-section for the first 70-meters and a 25-square meter cross-section for the remaining length. The range has 131 locations available as instrumentation sites and each location is separated by 1.5-meters. Presently, 50 of these sites are used to house fully instrumented orthogonal shadowgraph stations. At each of these stations, the maximum shadowgraph window (an imaginary circle in which a projectile will cast a shadow on two orthogonal reflective screens) is 2-meters in diameter. The orthogonal photographs of the model's shadow are then used to determine the spatial position and angular orientation of the test model at each of the 50-instrumented sites. The range is an atmospheric test facility where the temperature and the relative humidity are controlled to 22 ±1 °C and less than 55% respectively.

The Comprehensive Automated Data Reduction and Analysis System (CADRA)[2] is used to read the film and calculate the trajectory. The film is digitized using a high resolution scanning process. Automated image processing is done using CADRA.

A chronograph system provides the flight times for the projectile at each station. These times together with the spatial position and orientation obtained from the orthogonal photographs processed by the CADRA system provide the basic trajectory data for the subsequent analysis. These discrete times, positions, and orientations are then used by the Aeroballistic Research Facility Data Analysis System (ARFDAS)[3] to determine the aerodynamic coefficients and stability derivatives acting on the model during the observed flight.

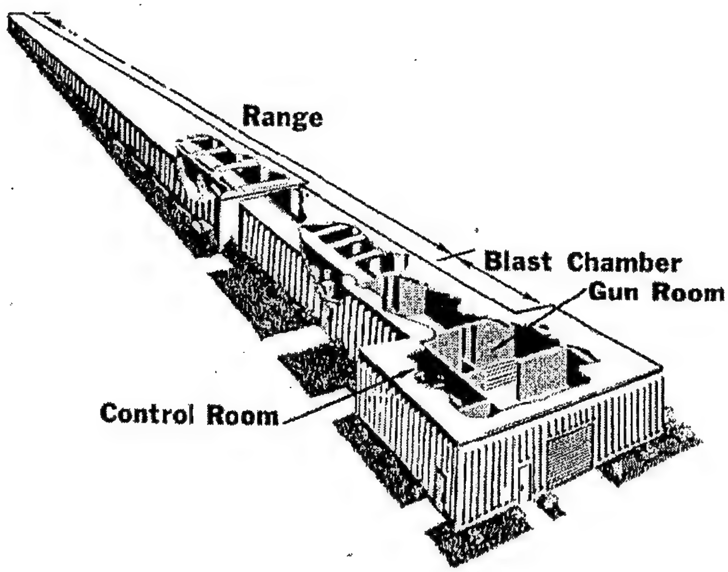

a) exterior view

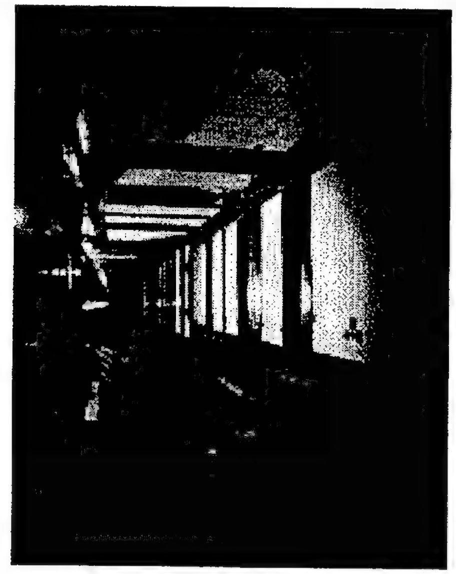

b) interior view

Figure 1. USAF Aeroballistic Research Facility (ARF), Eglin AFB, FL

2. Models and Test Conditions

A total of seven configurations were designed and tested for this effort. All configurations are designed to have an equivalent cross sectional area (i.e. reference area). In addition, the reference length used in the data analysis was common for all configurations. For missile configurations, the reference length is typically the diameter of the projectile. For the non-circular configurations, an "equivalent" diameter is used for the reference length such that the area of a circle based upon this diameter is equivalent to the non-circular area. However, since the cross-sectional areas were equivalent for all configurations, the reference length is the same for all configurations as well. This allows for one-to-one comparison of the data of each configuration to isolate the body alone influence.

The fin planform was identical for all configurations. This will further isolate the effects of the body alone. The test configurations are 8.08 calibers in length with a 2.2 caliber ogive. Figure 2 contains a schematic illustrating the test model configurations tested during this research program. The model dimensional details are provided in the following sections along with the aerodynamic data. A fin tab was attached to the fin tip trailing edge of one fin of each model in order to determine roll orientation. The flight data covered a Mach number range of 0.75 to 3.5. Table 1 lists the nominal physical properties for the configurations tested.

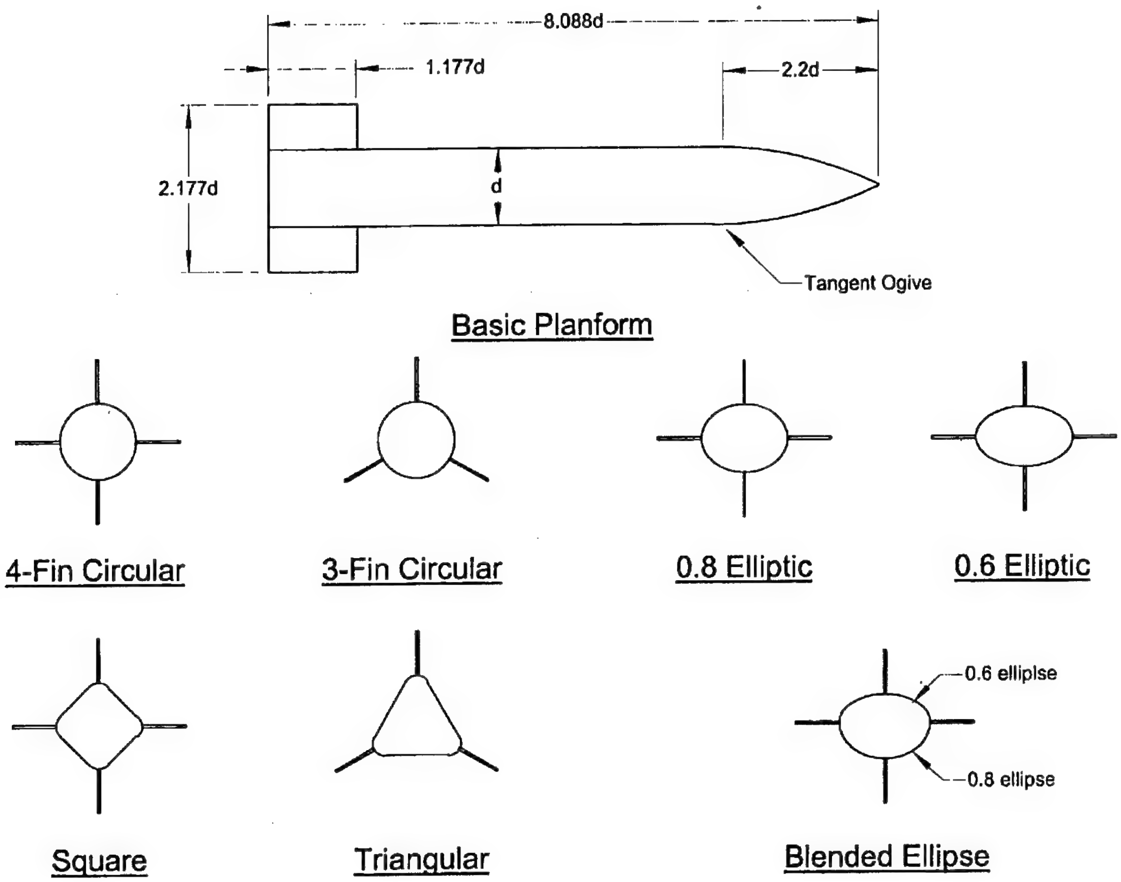

Figure 2. Model Cross Section Configurations

Table 1: Model Physical Properties

Configuration	Circular 4 Fin	Circular 3 Fin	0.8 Elliptical 4 Fin	0.6 Elliptical 4 Fin	Blended Elliptical 4 Fin	Square 4 Fin	Triangular 3 Fin
Diameter (d), mm	17	17	17	17	17	17	17
Length (L), mm	137.5	137.5	137.5	137.5	137.5	137.5	137.5
Mass, g	844	835	880	916	912	853	824
I_x, gram-cm^2	36.0	34.6	38.0	42.3	39.8	38.4	40.5
I_y, gram-cm^2	1270	1230	1355	1290	1410	1304	1230
C.G. location (X_{CG}), mm from nose	58.6	58.6	62.5	64.8	63.5	59.5	59.5
Number of ARF Trials	15	15	17	15	11	13	18

3. Aerodynamic Parameter Identification

Extraction of the aerodynamic coefficients and stability derivatives is the primary goal in analyzing the trajectories measured in the ARF. The process is summarized in Figure 3 and is accomplished by using ARFDAS[3]. ARFDAS incorporates a standard linear theory analysis[4,5] and a six degree-of-freedom (6DOF) numerical integration technique[6]. The 6DOF routine in ARFDAS incorporates the Maximum Likelihood Method (MLM)[7] to match the theoretical trajectory to the experimentally measured trajectory. The MLM is an iterative procedure that adjusts the aerodynamic coefficients to maximize a likelihood function. The use of this likelihood function eliminates the inherent assumption in least squares theory that the magnitude of the measurement noise must be consistent between dynamic parameters (irrespective of units). In general, the aerodynamics can be nonlinear functions of the angle of attack, Mach number, and aerodynamic roll angle. ARFDAS also has the ability to analyze nonaxisymmetric projectiles using a "body fixed" aerodynamic model. The "fixed plane" method for the analysis of axisymmetric projectiles is given in Appendix B and the "body fixed" method is described in Appendix C.

ARFDAS represents a complete ballistic range data reduction system capable of analyzing both symmetric and asymmetric bodies. The essential steps of the data reduction system are to: (a) assemble the dynamic range data (time, position, attitude), physical properties, and atmospheric conditions, (b) perform linear theory analysis, and (c) perform 6DOF analysis for final aerodynamics. These steps have been integrated into ARFDAS to provide the test engineer with a convenient and efficient means of interaction. At each step in the analysis, permanent records for each flight are maintained such that subsequent analysis with data modifications are much faster.

Each model fired in the ARF was initially analyzed separately, then combined in appropriate groups for simultaneous analysis using the multiple fit capability. This provides a common set of aerodynamics that match each of the separately measured position-attitude-time profiles. The multiple fit approach provides a more complete spectrum of angular and translational motion than would be available from any one trajectory considered separately. This increases the probability that the determined coefficients define the model's aerodynamics over the entire range of test conditions.

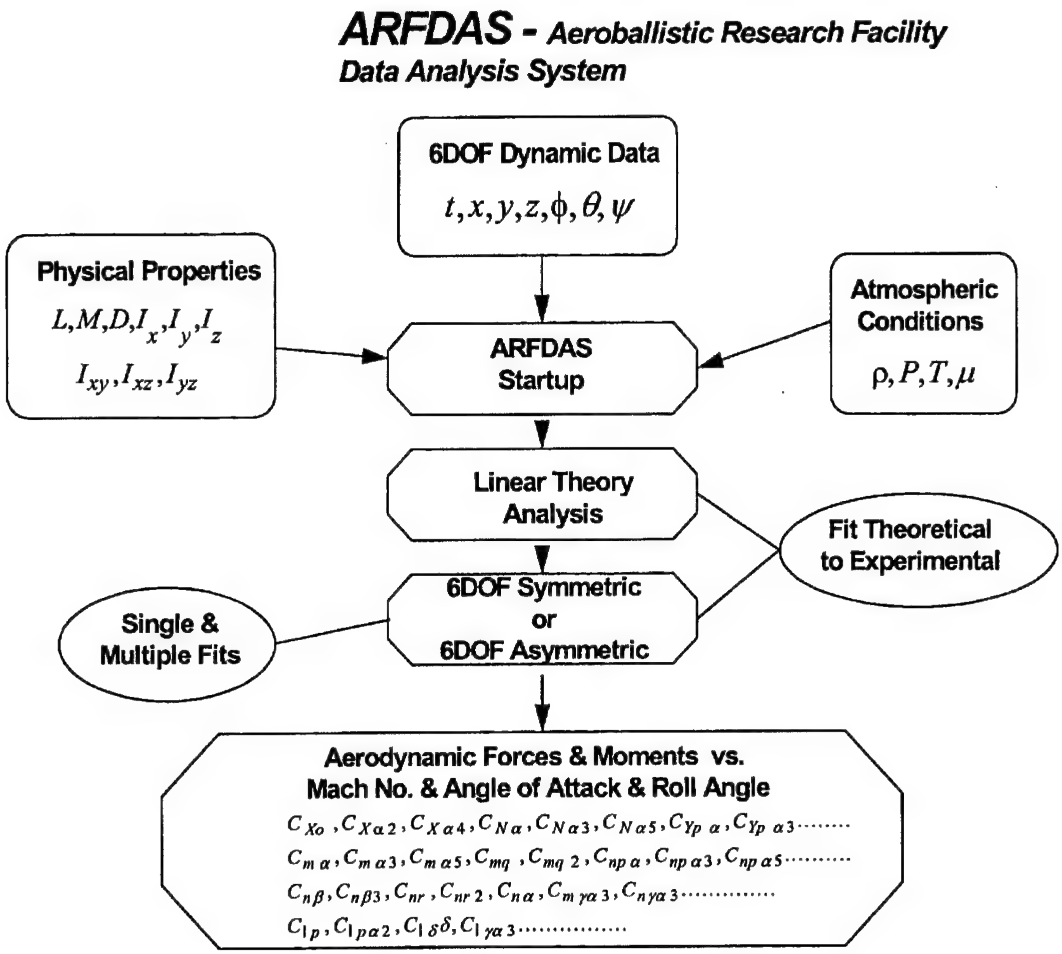

Figure 3. ARFDAS Aerodynamic Parameter Identification Process

INTENTIONALLY LEFT BLANK

SECTION III

RESULTS AND DISCUSSION

Aerodynamic force and moment coefficients and stability derivatives have been extracted from each set of free flight motion data measured in the ARF. The methodology includes both linear theory and six degree-of-freedom (6DOF) matching of the observed motions to determine the aerodynamics. The parameter identification methodology provides a best match to the experimentally measured motion by determining the aerodynamic forces and moments acting on the flight vehicle resulting in the measured motion.

The following sub-sections present the aerodynamic data determined from the ballistic range trials for each class of configuration: circular, elliptic, square, and triangular. Appendix D contains the tabular data of the physical properties, range conditions, and 6DOF aerodynamic results for each configuration. The 6DOF results contain both the single and multiple fit analysis data. It is believed that the multiple fit analysis represent the best estimates of the configurations aerodynamics since the combined trajectories contain more data over a wider range of angles of attack. The plots of aerodynamic data presented in the following sub-sections contain hollow and solid data symbols. A hollow symbol represents the result of a single fit analysis and a solid symbol represents the result of matching multiple flight trajectories to a common set of aerodynamics. It should be noted that the angular motion amplitude for most flights was very small. Such small amplitude angular and swerve motion diminish the accuracy of the resultant aerodynamic coefficients since its effect on matching the measured motion becomes less significant.

1. Circular Cross Section Configurations

Two circular cross-section configurations, a three-fin and a four-fin, were tested to provide a baseline for the other non-circular configurations. The four-fin configuration provides a baseline for the elliptic and square cross-section configurations and the three-fin provide a baseline for the triangular configuration. The two circular cross-section configurations had identical bodies and fin planform dimensions. Figure 4 contains a schematic of these two configurations.

Figure 5 presents the zero yaw axial force coefficient (C_{X_o}) versus Mach number as determined from the flight data for both the three-fin and four-fin circular cross section configurations. Since the only difference in the three and four fin models is the number of fins, the difference in drag seen in this figure is a direct result of the additional fin. The data indicate there is about a 5% difference in drag over the Mach number range from 0.6 through 3.2

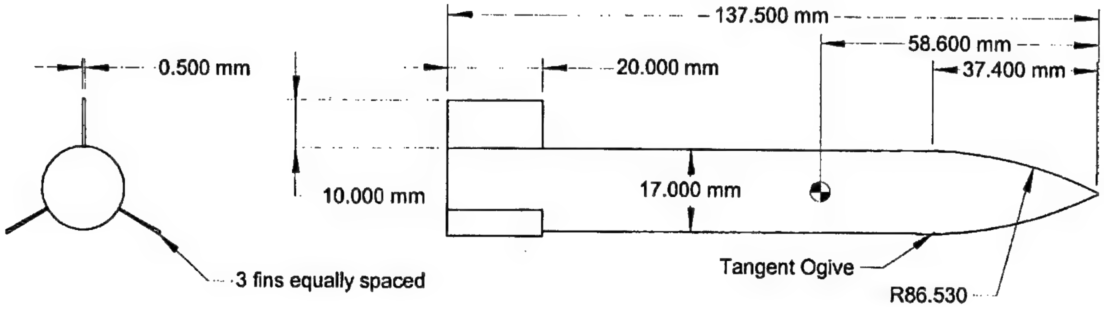

3-Fin Configuration

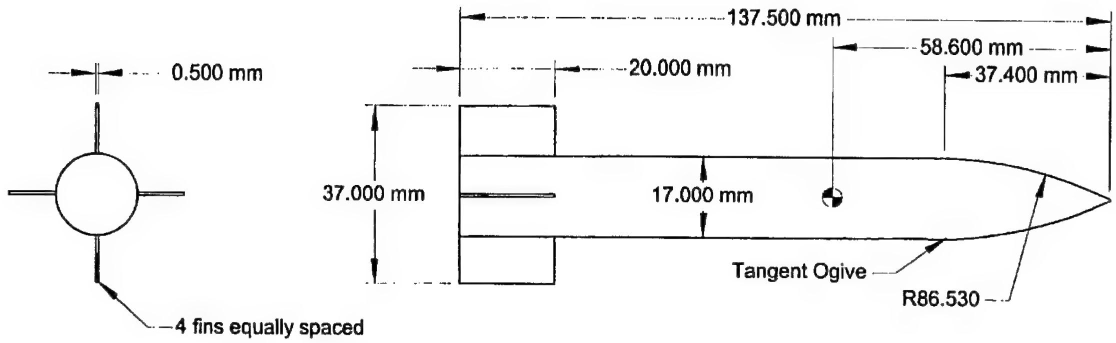

4-Fin Configuration

Figure 4. Three- Fin and Four-Fin Circular Configurations

Figure 6 shows the normal force coefficient derivative ($C_{N\alpha}$) versus Mach number for the three-fin and four-fin circular configurations. Here, the additional normal force resulting from the four versus three fins is quantified. There is about an 18% difference in normal force coefficient derivative at Mach 0.8. The difference increases to about 30% at Mach 1.4 and then decreases to about 5% at Mach 3.

Figure 7 contains the pitch moment coefficient derivative ($C_{m\alpha}$) as a function of Mach number. The difference in static stability for three versus four fins is clearly seen and is accurately determined. The difference in pitch moment coefficient derivative for the three-fin and four-fin configurations is about 20% over the entire Mach number range.

The variation of pitch damping moment coefficient (C_{mq}) versus Mach number is shown in Figure 8. Due to the small amplitude motion, it was difficult to accurately

determine the pitch damping moment. However, Figure 8 indicates that there was not a significant difference in the pitch damping with three versus four fins.

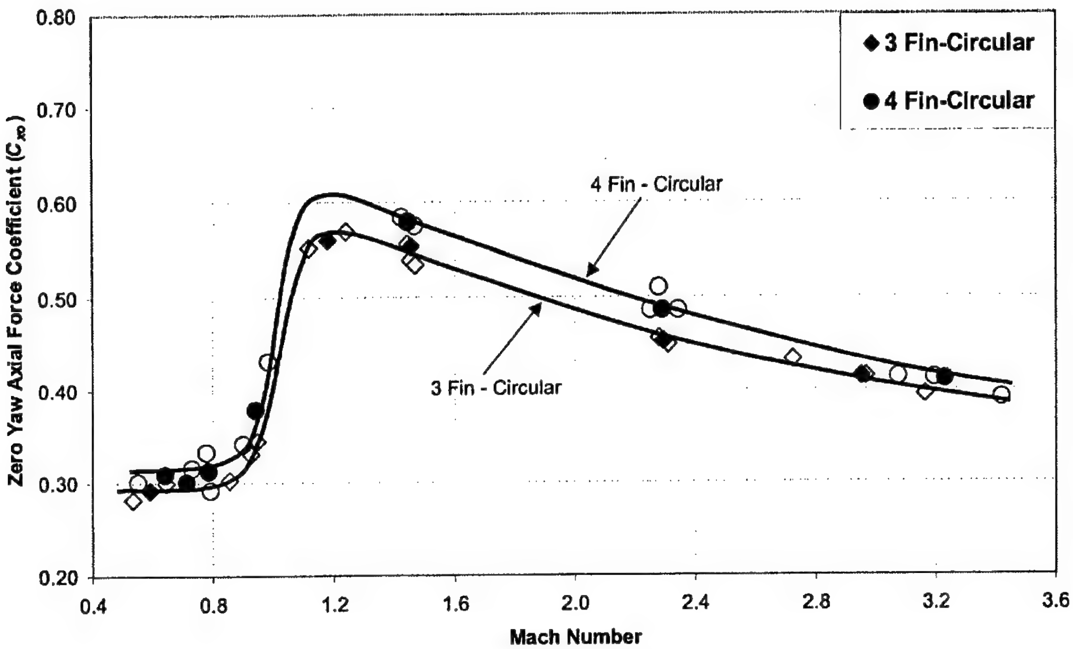

Figure 5. Zero Yaw Axial Force Coefficient versus Mach Number – Circular Cross Section Configurations

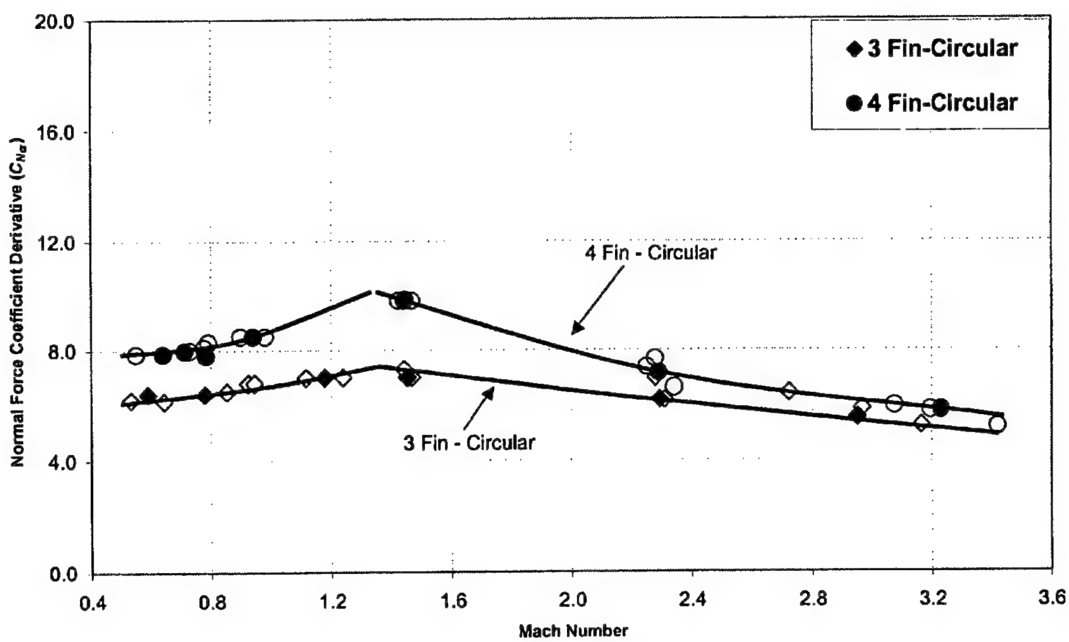

Figure 6. Normal Force Coefficient Derivative versus Mach Number – Circular Cross Section Configuration

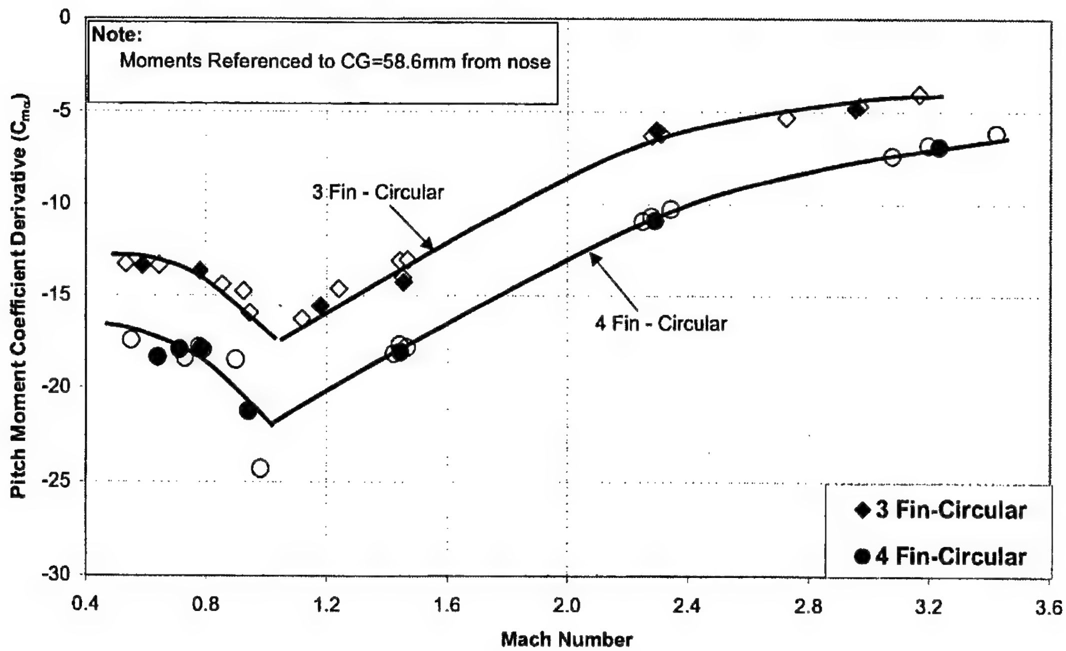

Figure 7. Pitch Moment Coefficient Derivative versus Mach Number – Circular Cross Section Configuration

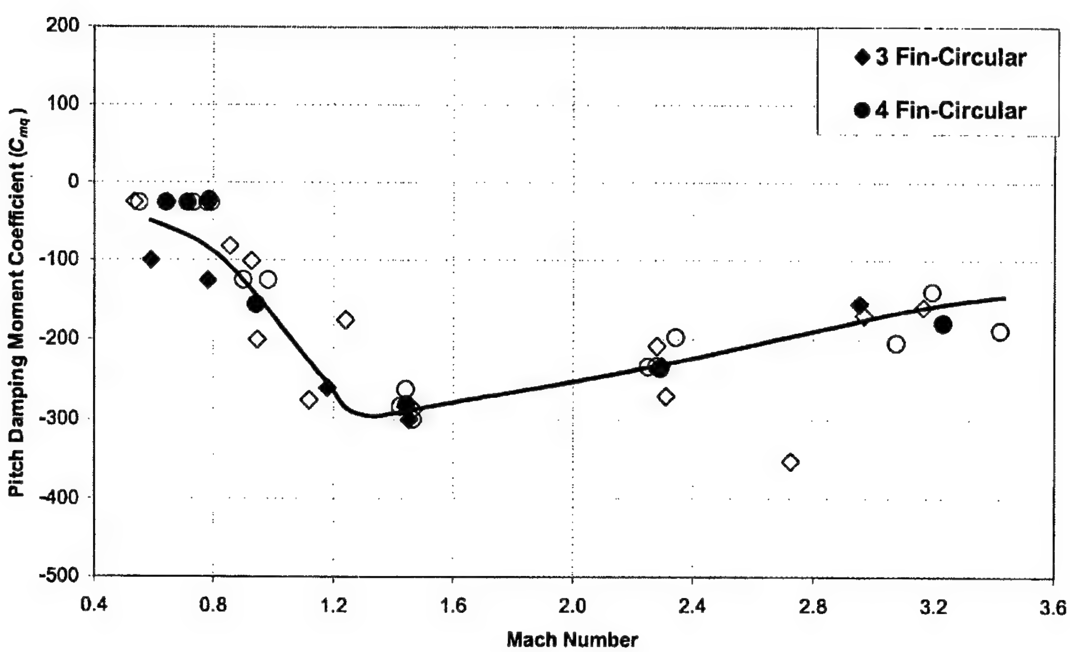

Figure 8. Pitch Damping Moment Coefficient versus Mach Number – Circular Cross Section Configuration

2. Elliptic Cross Section Configurations

Three elliptic cross-section configurations were tested in this effort. The first configuration had an elliptic cross section with a 0.8 eccentricity (ratio of minor diameter to major diameter) and the second had an elliptic cross section with a 0.6 eccentricity. The third configuration was a "blended" cross section that had a 0.6 eccentricity on the top half and a 0.8 eccentricity on the lower half. All three configurations contained four fins and are shown in Figure 9. As noted in Table 1, the center of gravity for each configuration was different.

Analysis of the flight data was done using the 6DOF "body fixed" equations of motion within ARFDAS[3] (see Appendix C). This allowed solving for unique force and moment coefficients in the pitch (alpha) and yaw (beta) planes (e.g. $C_{m\alpha} \neq C_{n\beta}$). The four-fin circular cross section configuration serves as a baseline for the elliptic configurations. Since all configurations tested in this effort have a common cross sectional area, the reference length and area are common to all configurations and this allows for direct comparison of the resultant data. However, there was variation in the CG locations of the various configurations and this will be important for moment coefficient comparisons.

The zero yaw axial force coefficient (C_{X_o}) versus Mach number as determined from the three elliptic cross section configuration flight data is contained in Figure 10. Also included for comparison are the 4-fin circular cross section results. Here again, the solid symbols represent "multiple fit" data versus single shot analysis. Although there is some scatter in the data in the Mach 0.8 regime, overall the data appear consistent for all configurations.

Figure 11 shows the pitch-plane (or alpha-plane) normal force coefficient derivative ($C_{Z\alpha}$) versus Mach number. The data of Figure 11 show the increase in body lift generated with the elliptic body in the plane of the major diameter.

Figure 12 shows the yaw-plane (or beta-plane) yaw force coefficient derivative ($C_{Y\beta}$) versus Mach number. The yaw-plane force coefficient derivative results have more scatter than the pitch-plane force coefficient derivative as seen in Figure 11 due to low amplitude motion. However, the trend shows decreased lift in the yaw-plane (minor diameter) versus the pitch-plane.

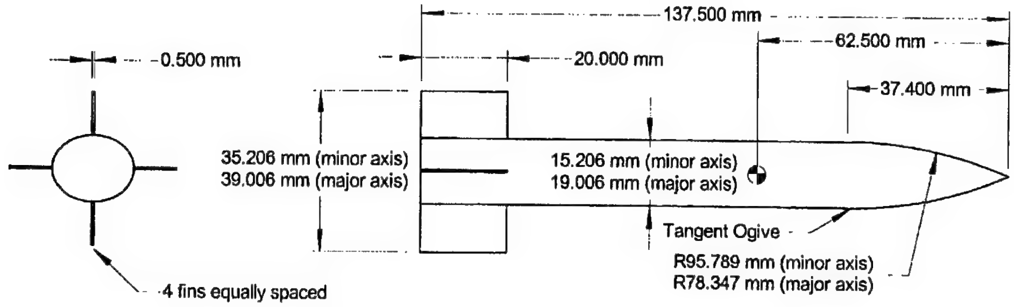

0.8 Elliptic Configuration

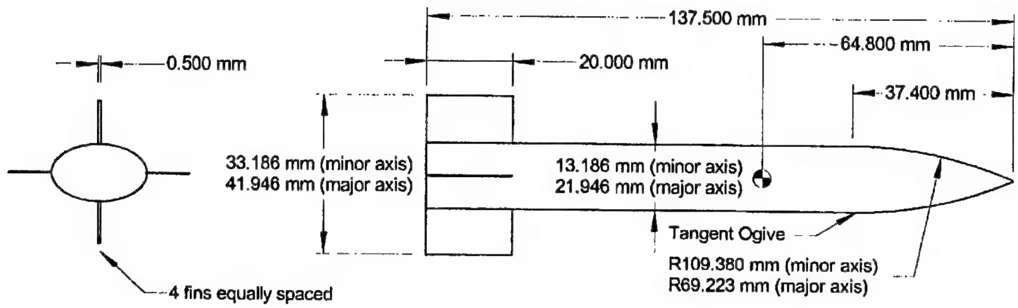

0.6 Elliptic Configuration

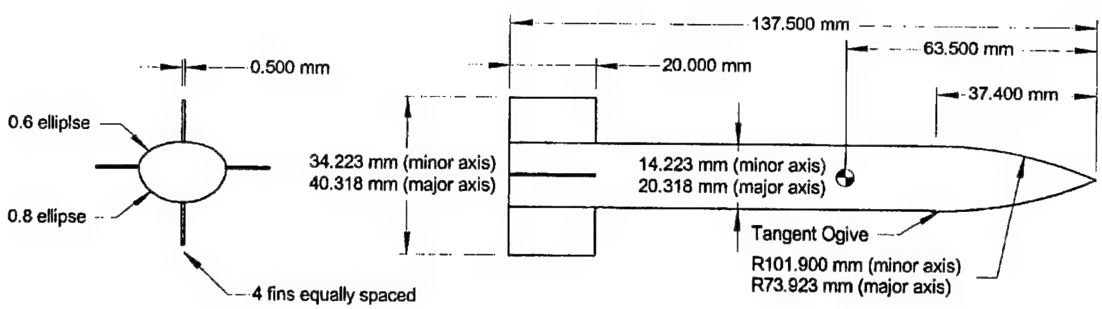

Blended Elliptic Configuration

Figure 9. Elliptic Cross Section Configurations

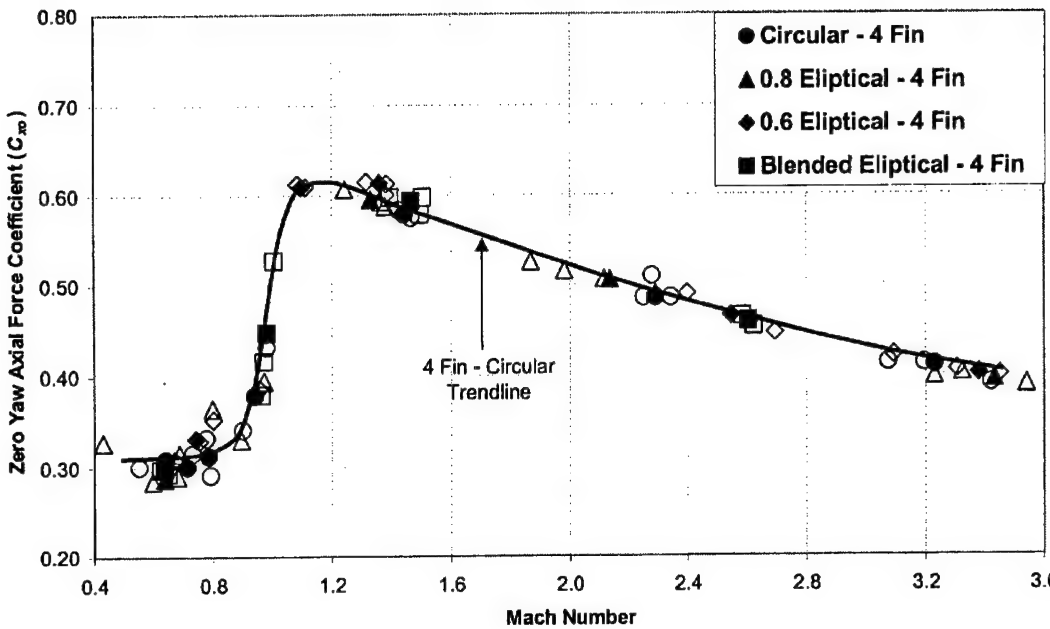

Figure 10. Zero Yaw Axial Force Coefficient versus Mach Number – Elliptic Cross Section Configurations

Figure 13 contains the pitch (alpha-plane) moment coefficient derivative ($C_{m\alpha}$) as a function of Mach number as extracted from the ARF flight data measurements. As indicated, the moment references were the individual CG locations for each configuration. The Mach number trends are similar as would be expected. However, to make direct comparisons between the configurations, the moment reference should be common for each configuration. Figure 14 contains the same results with the moments adjusted to a common body reference location coincident with the CG location for the four-fin circular cross section model. The moment adjustments were done using the following equation[6]:

$$C_{m\alpha}(58.6mm\ \text{Ref}) = C_{m\alpha}(CG\ \text{Ref}) + C_{Z\alpha}\left(\frac{58.6 - CG\ \text{Ref}}{d}\right) \quad (1)$$

Comparing the pitching moment results for all three elliptic configurations and the circular cross section (Figure 14), the differences are small with the possible exception of the transonic Mach regime. This would imply that the increase in Normal force for the elliptic shapes was coupled with a forward movement of the center of pressure location resulting in an equivalent pitching moment.

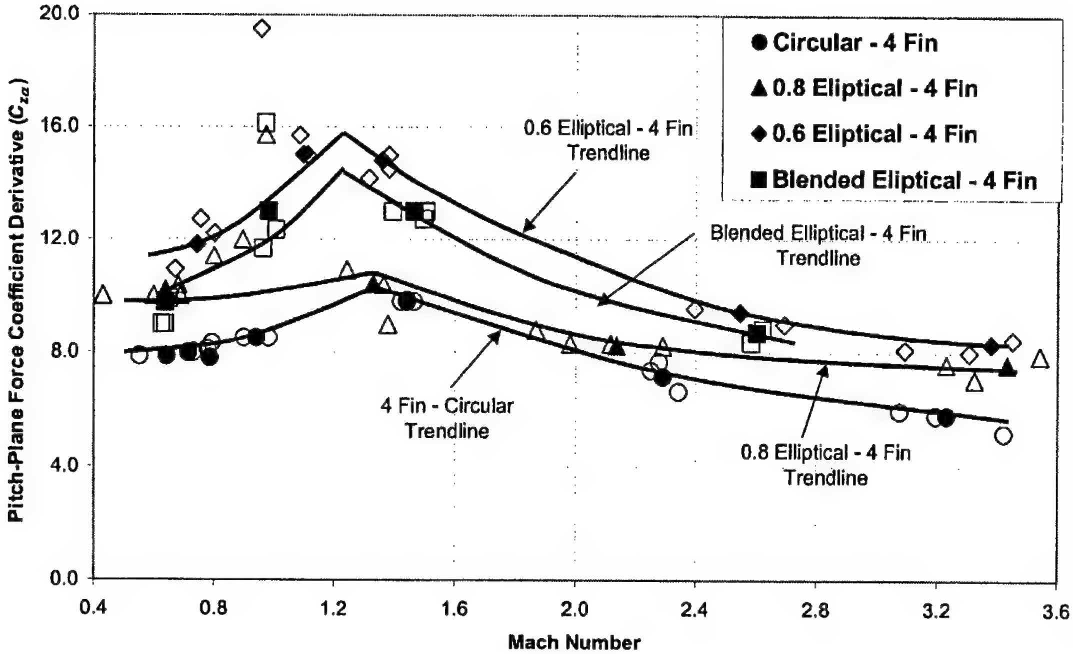

Figure 11. Pitch-Plane (Alpha-Plane) Force Coefficient Derivative versus Mach Number - Elliptic Cross Section Configurations

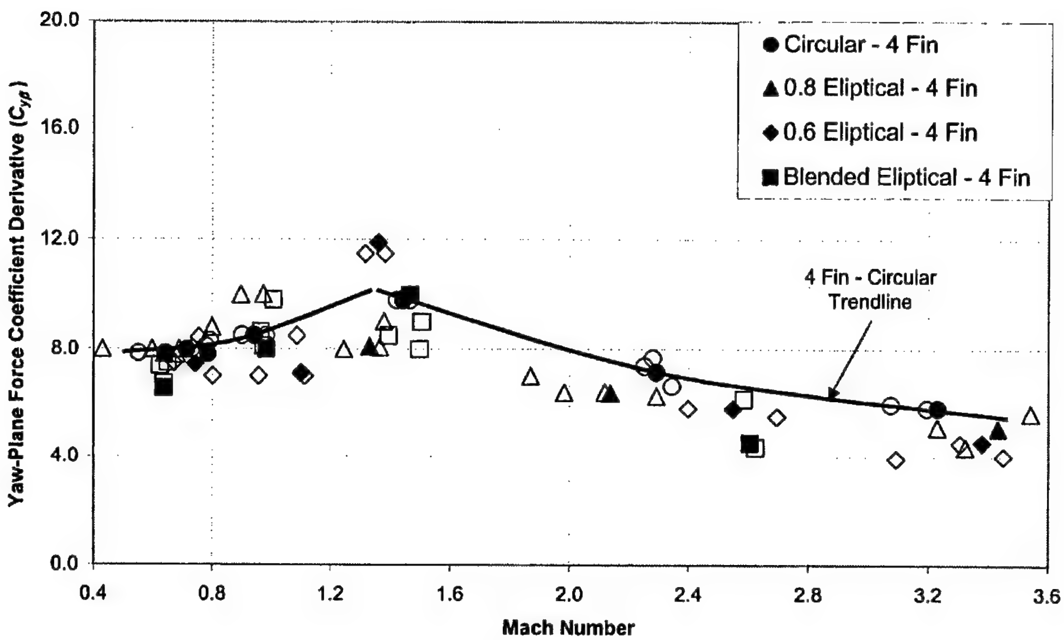

Figure 12. Yaw-Plane (Beta-Plane) Normal Force Coefficient Derivative versus Mach Number - Elliptic Cross Section Configurations

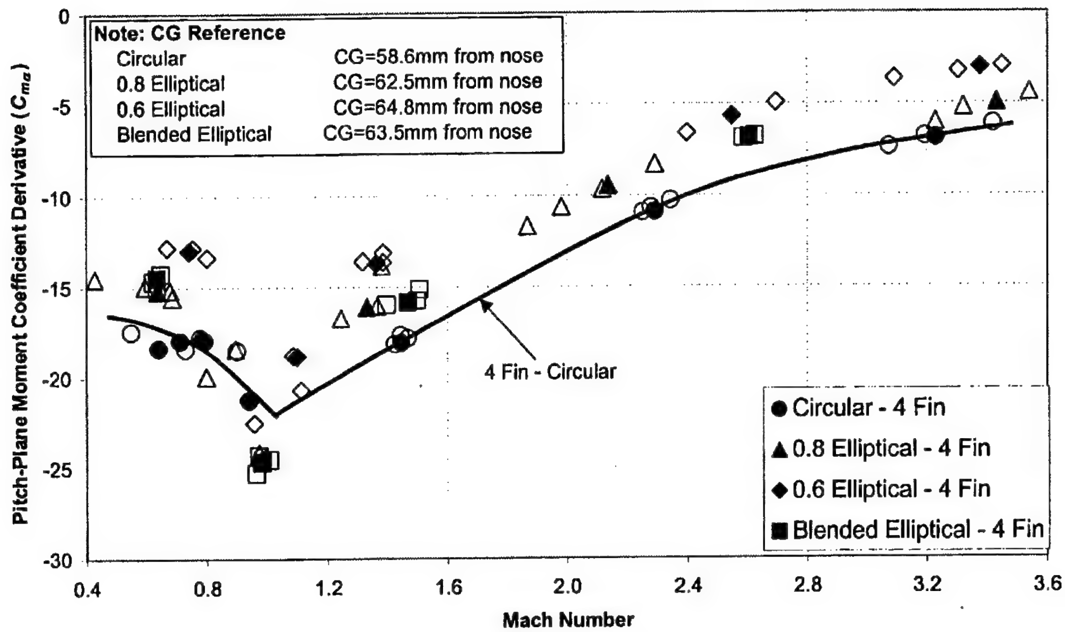

Figure 13. Pitch-Plane (Alpha-Plane) Moment Coefficient Derivative versus Mach Number - Elliptic Cross Section Configurations

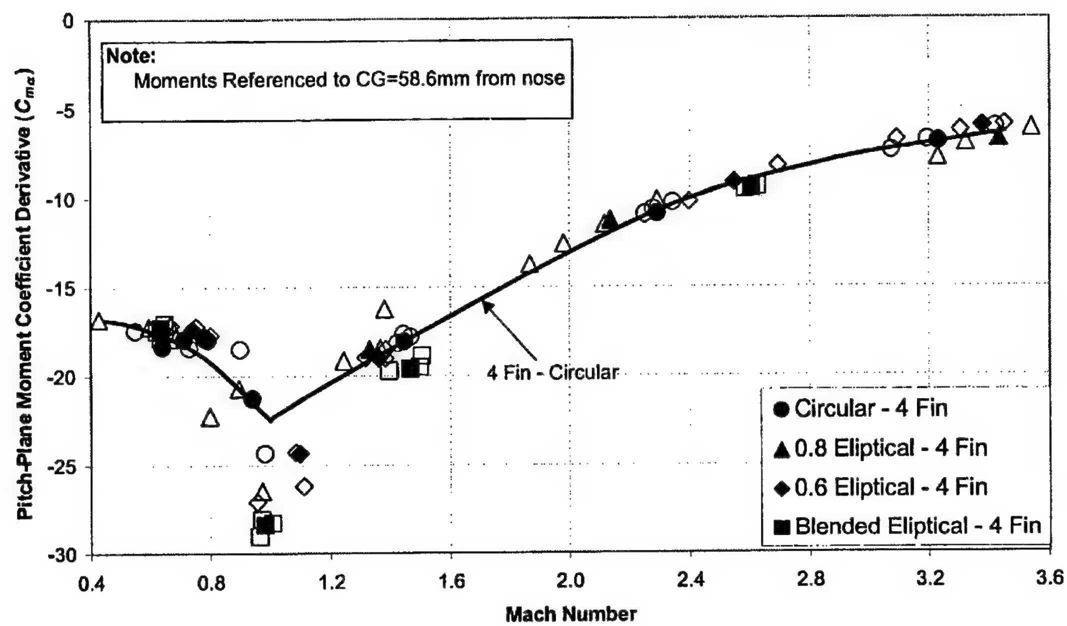

Figure 14. Pitch-Plane (Alpha-Plane) Moment Coefficient Derivative versus Mach Number with Common Moment Reference - Elliptic Cross Section Configurations

Figure 15 contains the yaw (beta-plane) moment coefficient derivative ($C_{n\beta}$) as a function of Mach number as extracted from the free-flight data measurements. Here again, as in the case for the pitch plane, the moment references were the individual CG locations for each configuration. The yaw moment coefficient derivatives were adjusted to a common body axial location and the results are plotted in Figure 16.

Comparing the yawing moment results for all three elliptic configurations and the circular cross section (Figure 16), the differences are small with the possible exception of the transonic Mach regime as is the case for the moment in the alpha-plane. However, the yaw force (beta plane) showed a slight decrease as compared to the circular cross section. This would imply that the decrease in yaw force for the elliptic shapes was coupled with a rearward movement of the center of pressure location resulting in an equivalent yawing moment.

The damping moment coefficients in the alpha plane (C_{mq}) and the beta plane (C_{nr}) extracted from the flight data are plotted in Figure 17 and Figure 18. The qualitative trends show a small decrease in the damping moment in the beta plane (minor diameter).

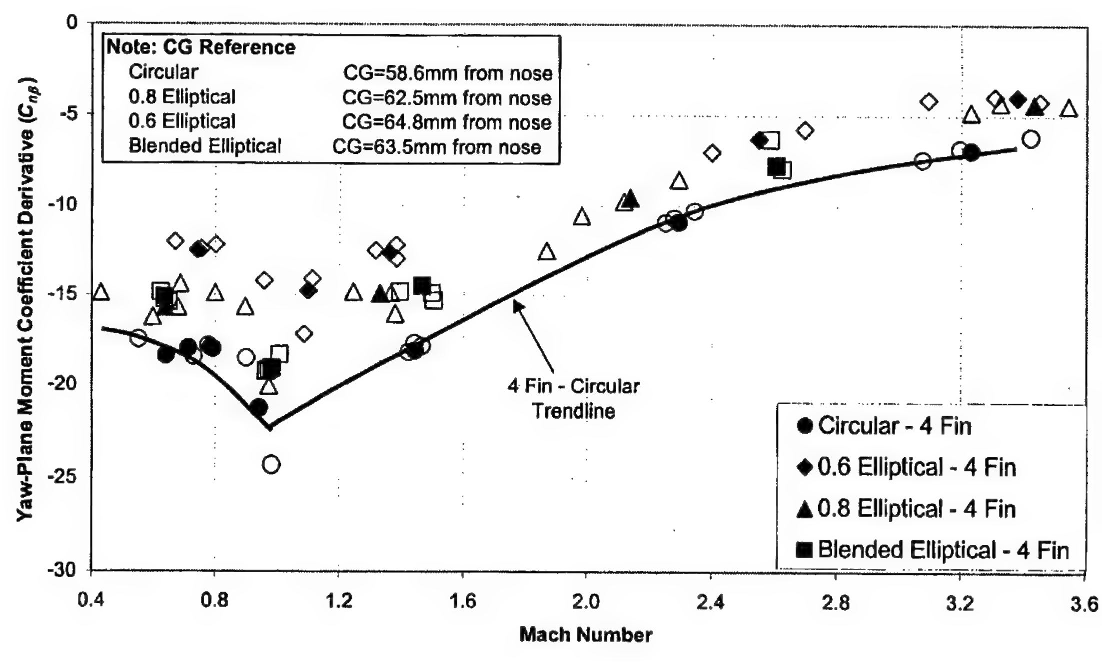

Figure 15. Yaw-Plane (Beta-Plane) Moment Coefficient Derivative versus Mach Number - Elliptic Cross Section Configurations

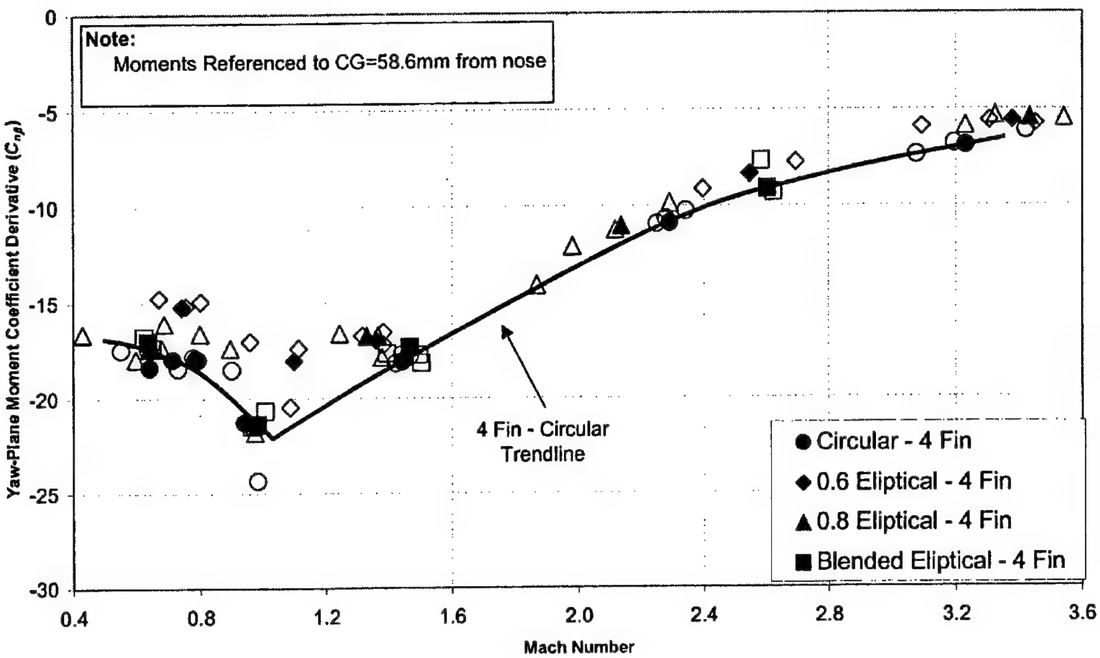

Figure 16. Yaw-Plane (Beta-Plane) Moment Coefficient Derivative versus Mach Number with Common Moment Reference - Elliptic Cross Section Configurations

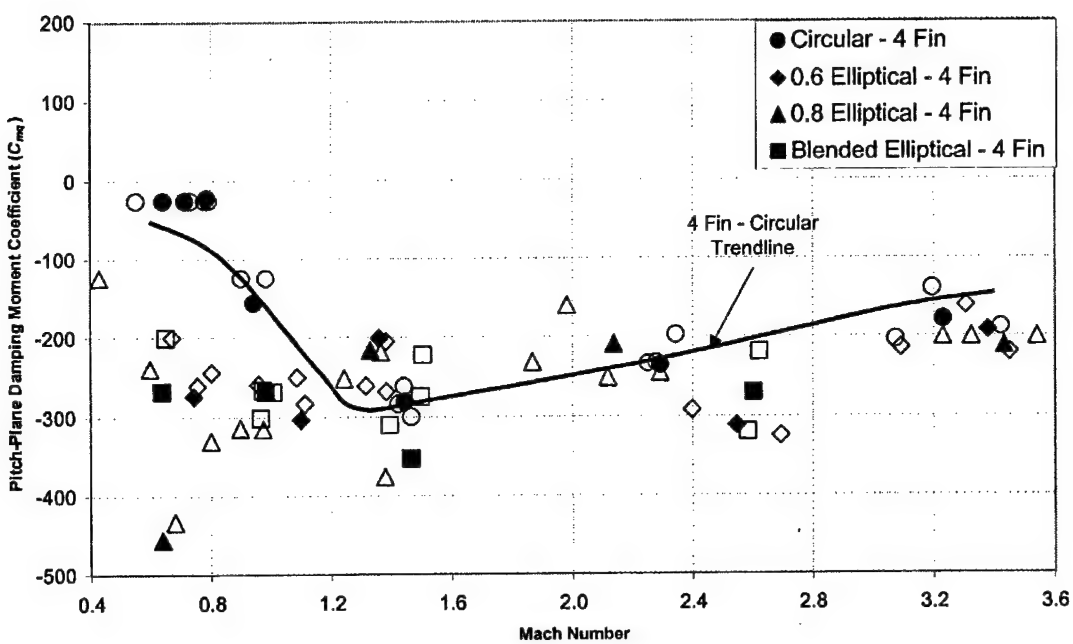

Figure 17. Pitch-Plane (Alpha-Plane) Damping Moment Coefficient versus Mach Number - Elliptic Cross Section Configurations

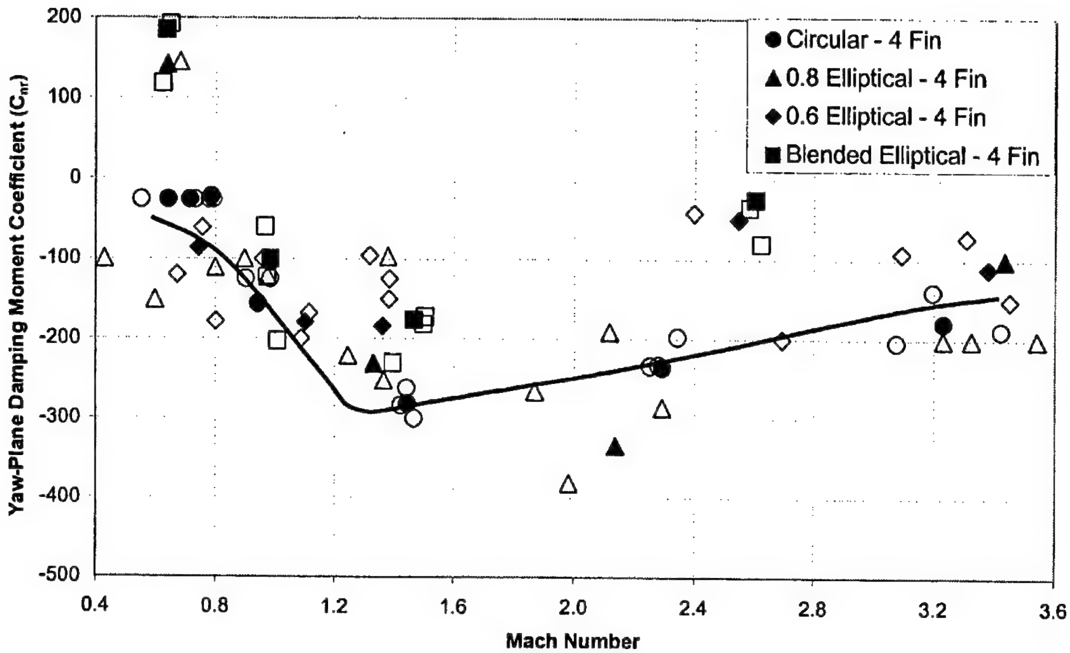

Figure 18. Yaw-Plane (Beta-Plane) Damping Moment Coefficient versus Mach Number - Elliptic Cross Section Configurations

The center of pressure can be found via the following equation[6]:

$$\frac{X_{c.p.}}{L} = \frac{X_{CG}}{L} - \frac{C_{m\alpha}}{C_{N\alpha}} \frac{d}{L}. \qquad (2)$$

The center of pressure for the pitch-plane (alpha-plane) was computed based on the resulting normal force and pitch moment coefficients in the pitch-plane. These results are presented in Figure 19 on a scale consistent with the total body length. The center of pressure for the yaw-plane (beta-plane) was computed in a similar fashion based on the resulting yaw force and yaw moment coefficients in the beta plane. These results are presented in Figure 20 on a scale consistent with the total body length.

In Figure 21, these center of pressure results in the pitch-plane, for the multiple fit results only, are plotted on an expanded scale. This provides a detailed comparison of the most accurate results showing a slight forward movement of the normal force center of pressure (alpha plane) with the elliptic configurations. Figure 22 shows the center of pressure results for the yaw-plane on the same expanded scale for that of the pitch-plane. In general, the center of pressure in the yaw-plane is about 5% of the body length aft of the center of pressure in the pitch-plane. However, the data is not refined to make an accurate quantitative measurement.

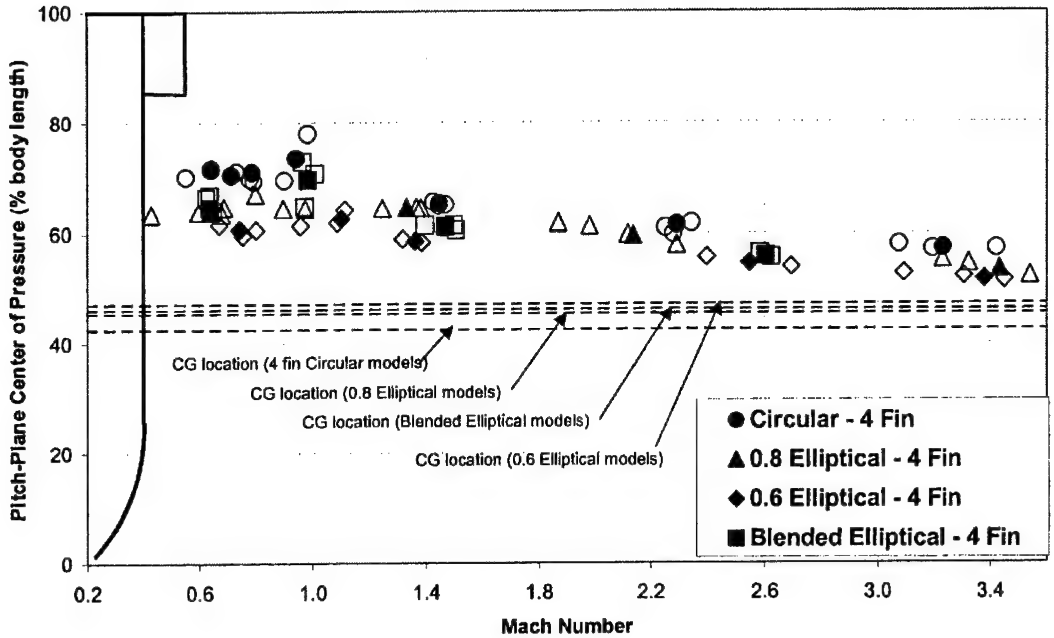

Figure 19. Pitch-Plane (Alpha-Plane) Center of Pressure Location versus Mach Number – Elliptic Cross Section Configurations

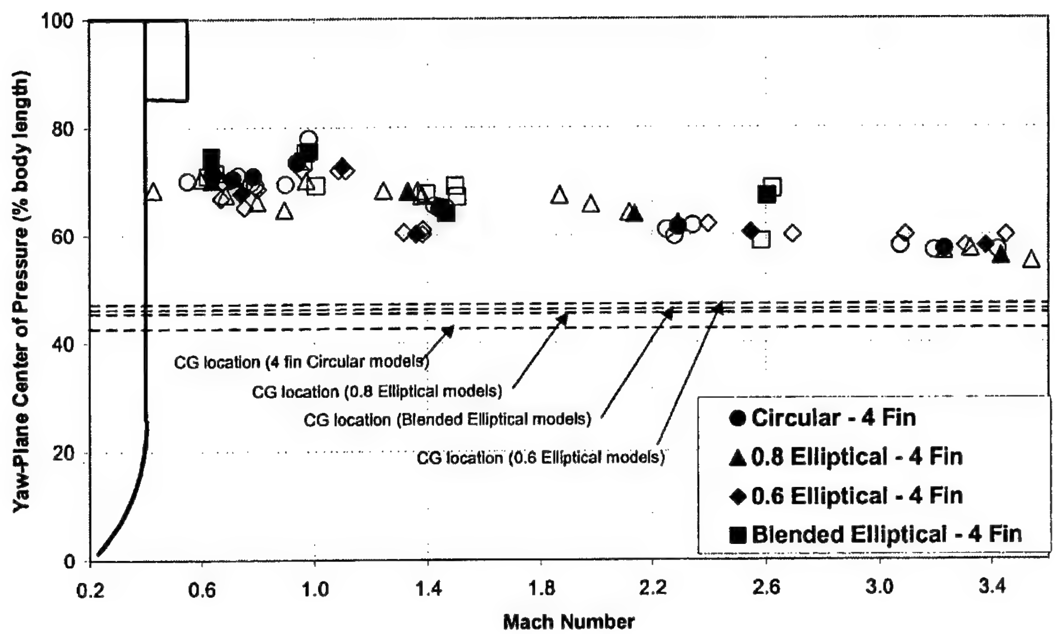

Figure 20. Yaw-Plane (Beta-Plane) Center of Pressure Location versus Mach Number – Elliptic Cross Section Configurations

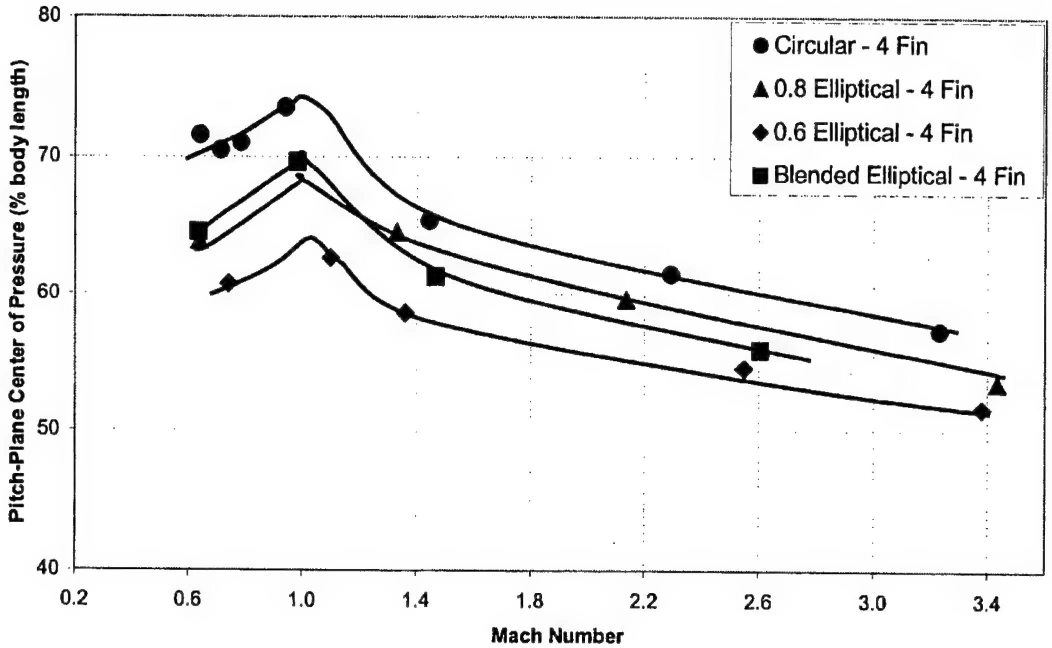

Figure 21. Pitch-Plane (Alpha-Plane) Center of Pressure Location versus Mach Number (enhanced scale) – Elliptic Cross Section Configurations

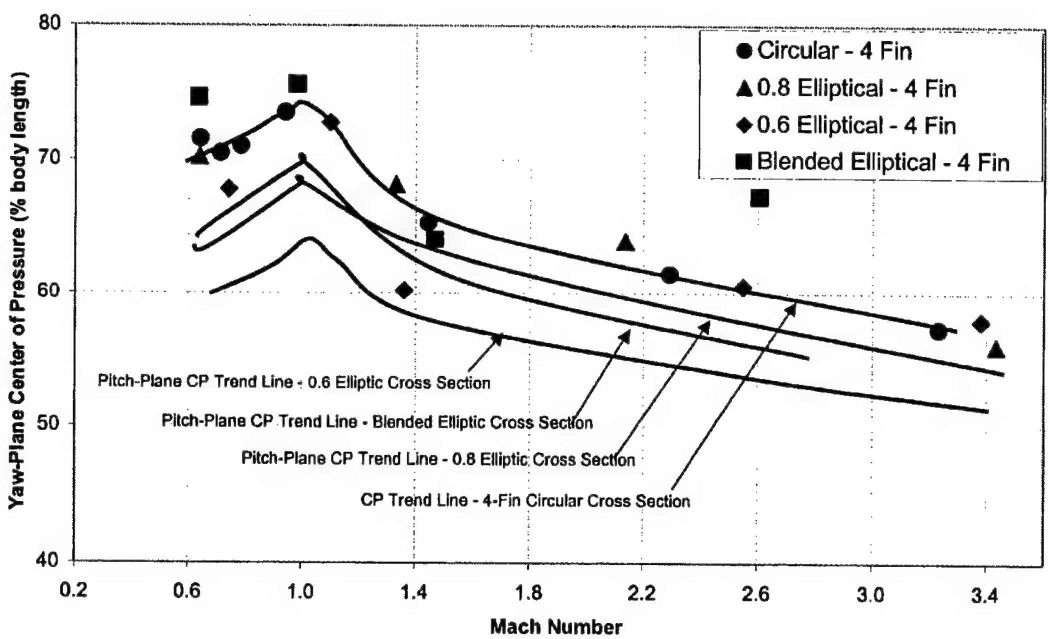

Figure 22. Yaw-Plane (Beta-Plane) Center of Pressure Location versus Mach Number (enhanced scale) – Elliptic Cross Section Configurations

3. Square Cross Section Configurations

One square cross section configuration was tested in this effort. The aerodynamic data from this configuration will be compared with the four-fin circular configuration data. Figure 23 depicts the four-fin square cross section configuration tested in this effort. It should be noted from Figure 23 that the square section blends with a segment of the ogive. In addition, the corners of the square are rounded as shown in Figure 23. This data was analyzed using the fixed plane equations of motion in ARFDAS.

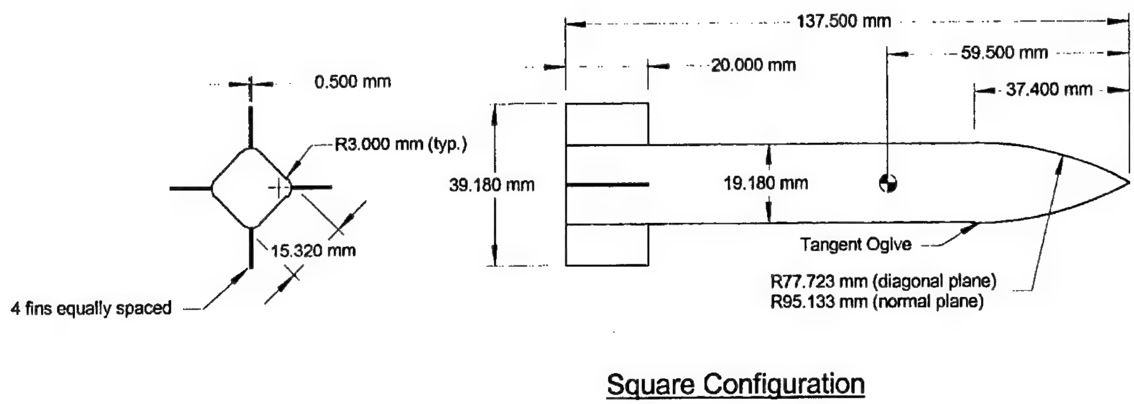

Figure 23. Square Body Cross Section Configuration

Figure 24 contains the zero yaw axial force coefficient results extracted from the flight data. The supersonic drag for the square cross section is about 7 percent higher than the circular cross section but at subsonic velocities, there is very little difference in the data.

Figure 25 contains the normal force coefficient derivative results for the square cross section configuration. Relative to the four-fin circular cross section, the normal force is larger in the supersonic regime, only slightly larger in the transonic regime, and about the same subsonic.

The pitch moment coefficient derivative results are presented in Figure 26. The square cross section models resulted in about a 10% increase in pitch moment coefficient derivative versus the four-fin circular configuration in the supersonic regime. The difference is smaller, about 5% in the subsonic regime.

The pitch damping moment coefficient derivative results are presented in Figure 27. Here only a slight change from the four-fin circular configuration is noticed.

The normal force center of pressure was computed based on the extracted normal force and pitching moment (see equation 2). The results are plotted in Figure 28. Differences in center of pressure location between the two configurations are small.

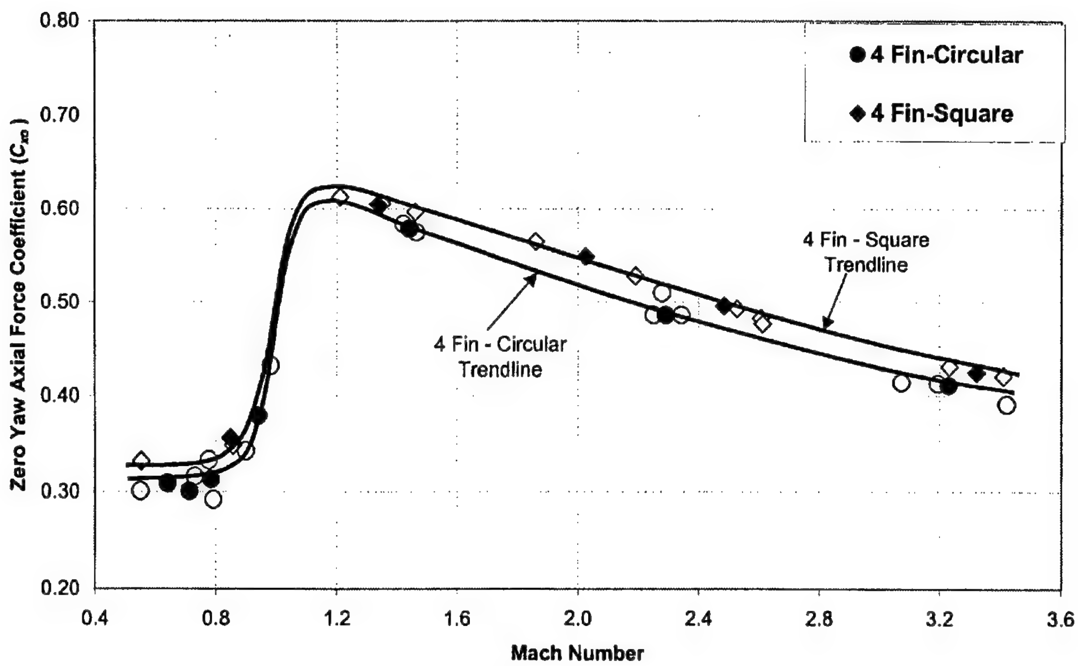

Figure 24. Zero Yaw Axial Force Coefficient versus Mach Number – Square Cross Section Configuration

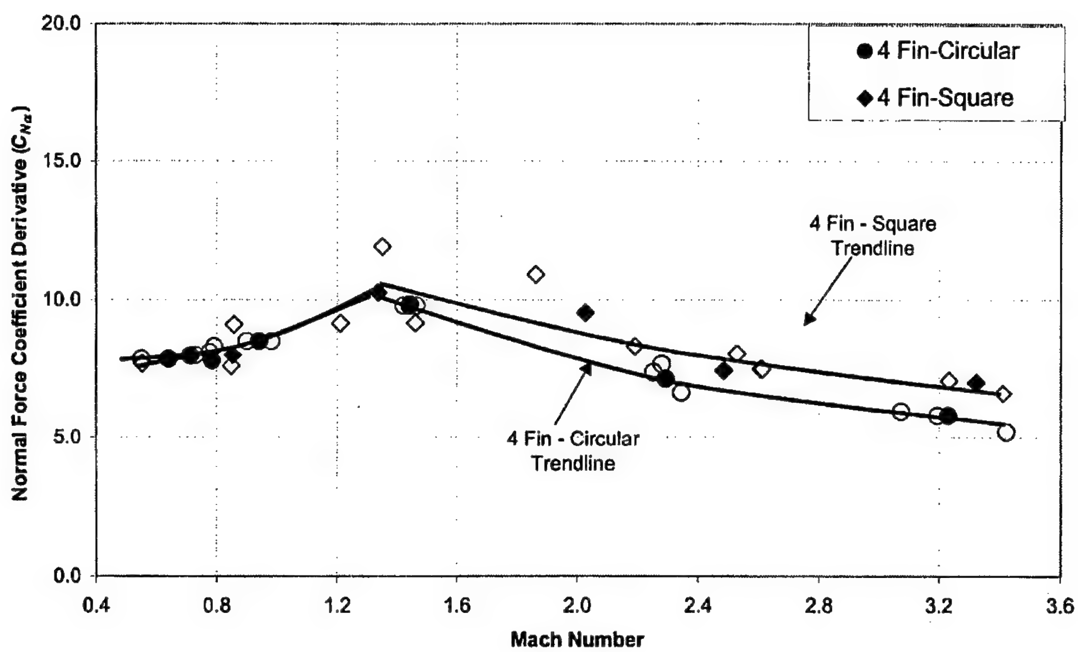

Figure 25. Normal Force Coefficient Derivative versus Mach Number – Square Cross Section Configuration

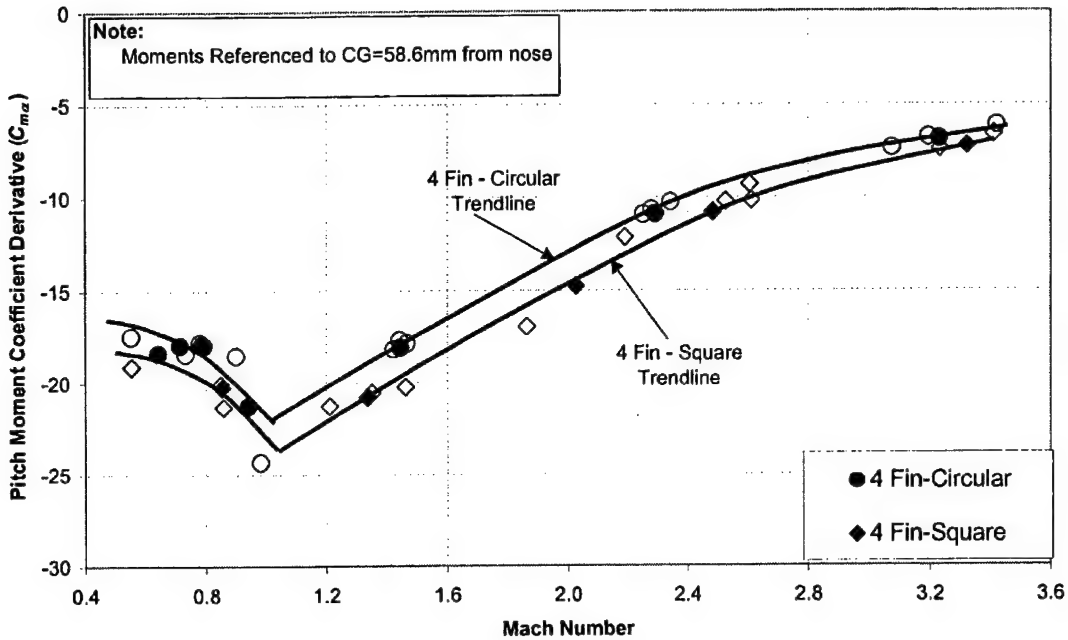

Figure 26. Pitch Moment Coefficient Derivative versus Mach Number – Square Cross Section Configuration

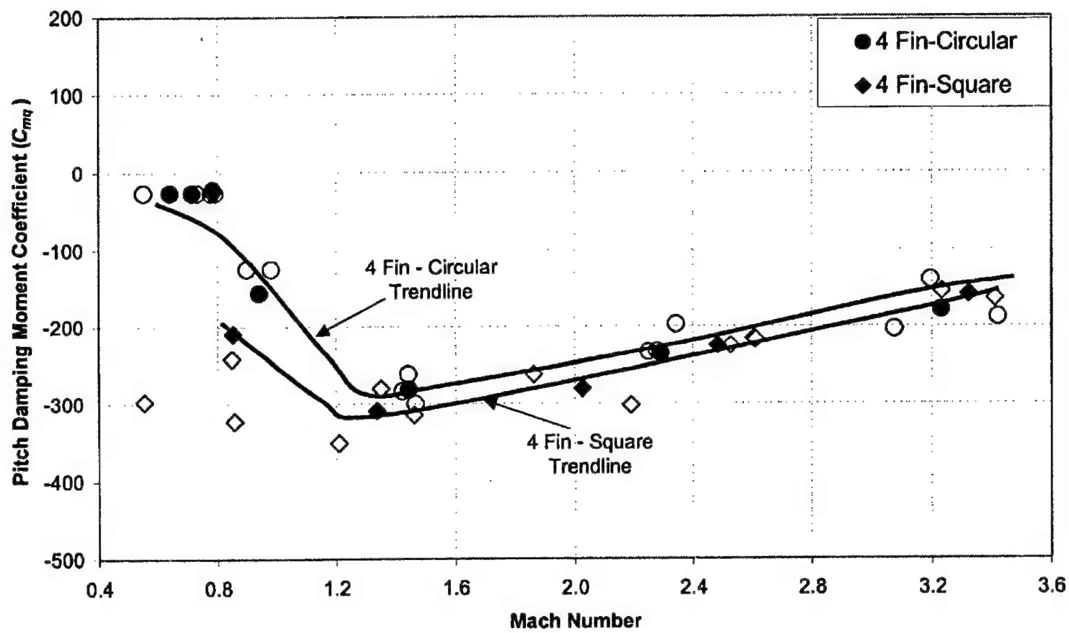

Figure 27. Pitch Moment Damping Coefficient versus Mach Number – Square Cross Section Configuration

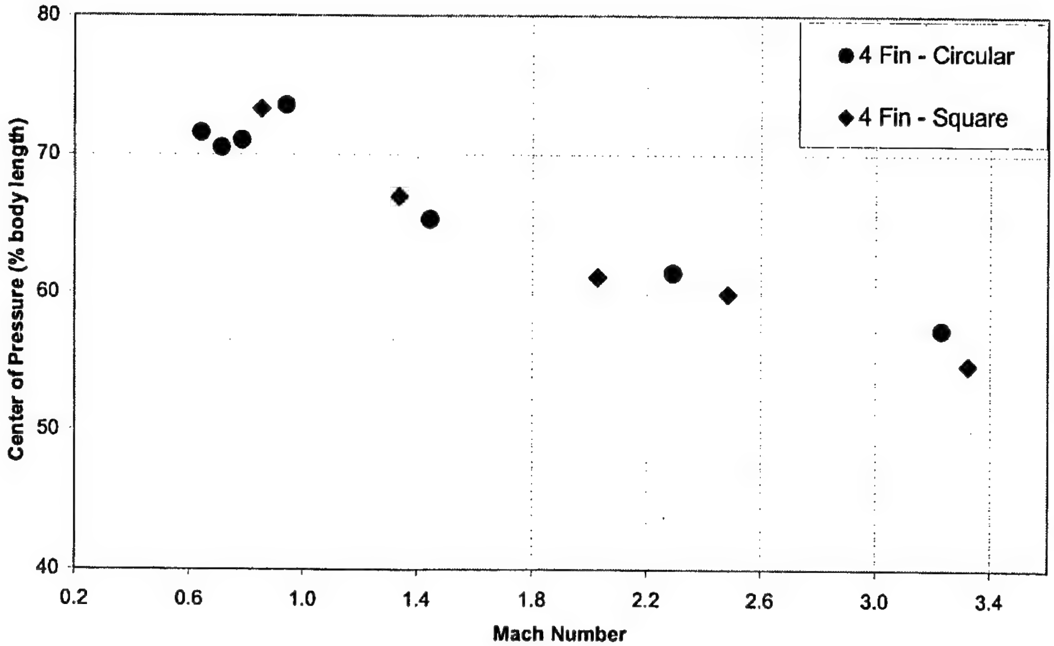

Figure 28. Center of Pressure Location versus Mach Number (enhanced scale) – Square Cross Section Configuration

4. Triangular Cross Section Configurations

Figure 29 depicts the three-fin triangular cross section configuration tested in this effort. The results presented are compared against the three-fin circular cross section. It should be noted from Figure 29 that the triangular section blends with a segment of the ogive. In addition, the corners of the triangular cross section are rounded.

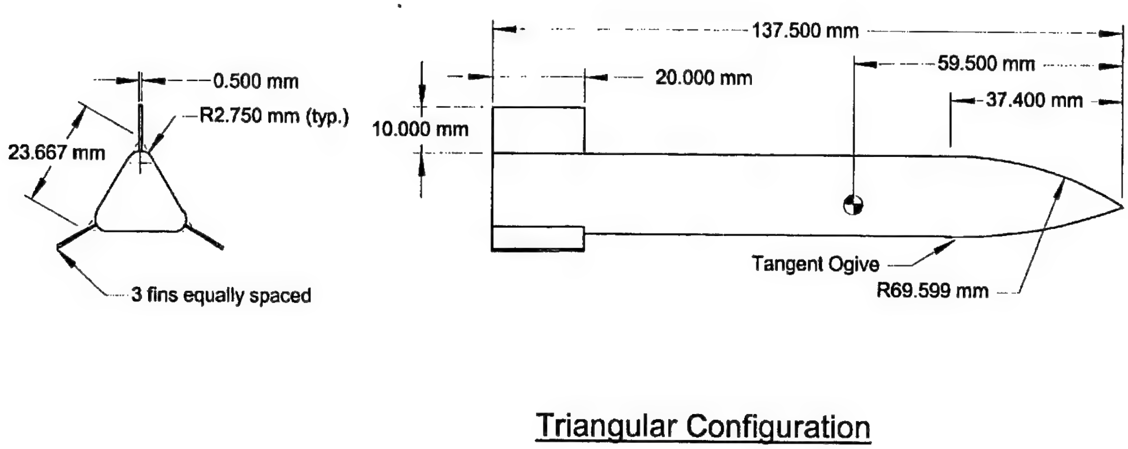

Figure 29. Triangular Body Cross Section Configuration

Initially, the extraction of the aerodynamics was performed with the body fixed equations of motion and asymmetric aerodynamic model. Analysis of the data was also done using the fixed plane model. The quality of the match to the measured motion was equivalent for both. The conclusion is that the differences (e.g. $C_{m\alpha}$ versus $C_{n\beta}$) do not have a measurable effect on the low amplitude motion measurements from these flights in the ARF. Therefore, additional flights with induced motion for larger amplitudes are required to adequately define the aerodynamic asymmetries.

Figure 30 contains the axial force coefficient results extracted from the flight data. The transonic and low supersonic drag for the triangular cross section is higher than the circular cross section.

Figure 31 contains the normal force coefficient derivative results. The normal force experimental results for the triangular configuration show more scatter than the circular configuration as a result of the low motion amplitude. However, the increase in normal force resulting from the triangular cross section is quantified.

The pitching moment coefficient derivative results are presented in Figure 32.

The pitching moment for the triangular cross section is larger throughout the Mach range, but particularly below Mach 2.5.

The pitch damping results are presented in Figure 33. Differences between the pitch damping coefficients are considered within the measurement noise relative to the effect of matching the observed motion.

The normal force center of pressure was computed based on the extracted normal force and pitching moment via equation 2. The results are plotted in Figure 34. The center of pressure for the triangular cross section is about 0.5 calibers forward as compared to the circular cross section.

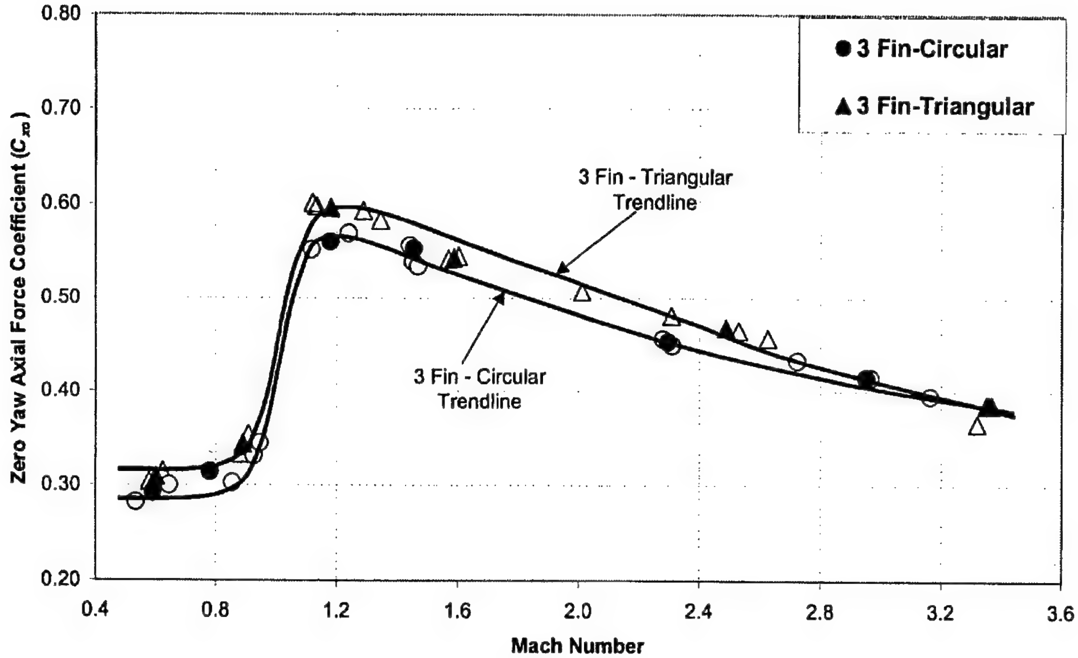

Figure 30. Zero Yaw Axial Force Coefficient versus Mach Number – Triangular Cross Section Configuration

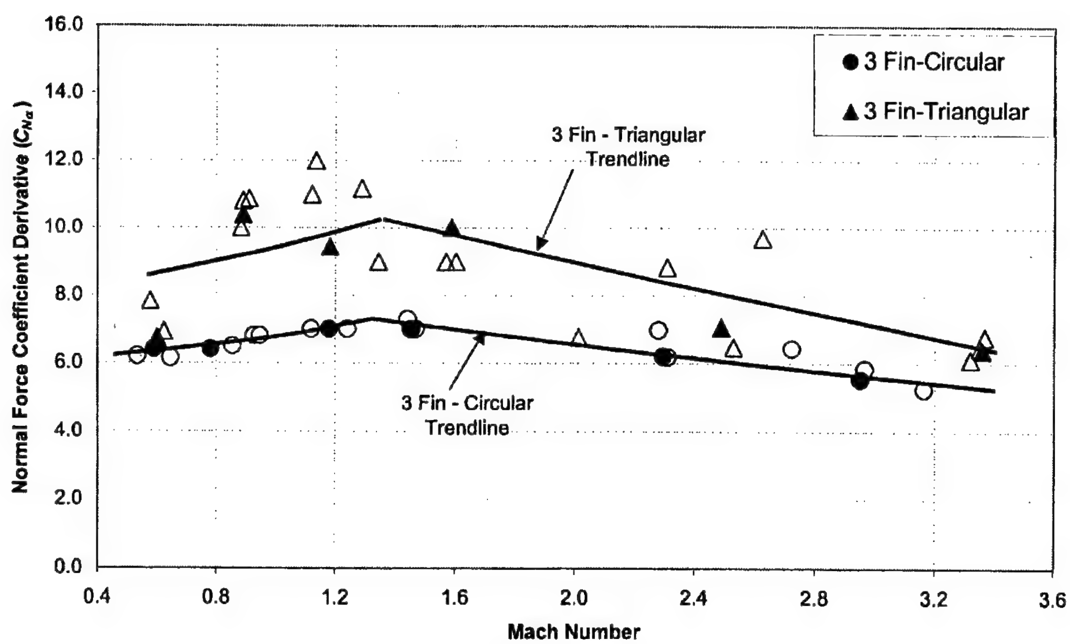

Figure 31. Normal Force Coefficient Derivative versus Mach Number – Triangular Cross Section Configuration

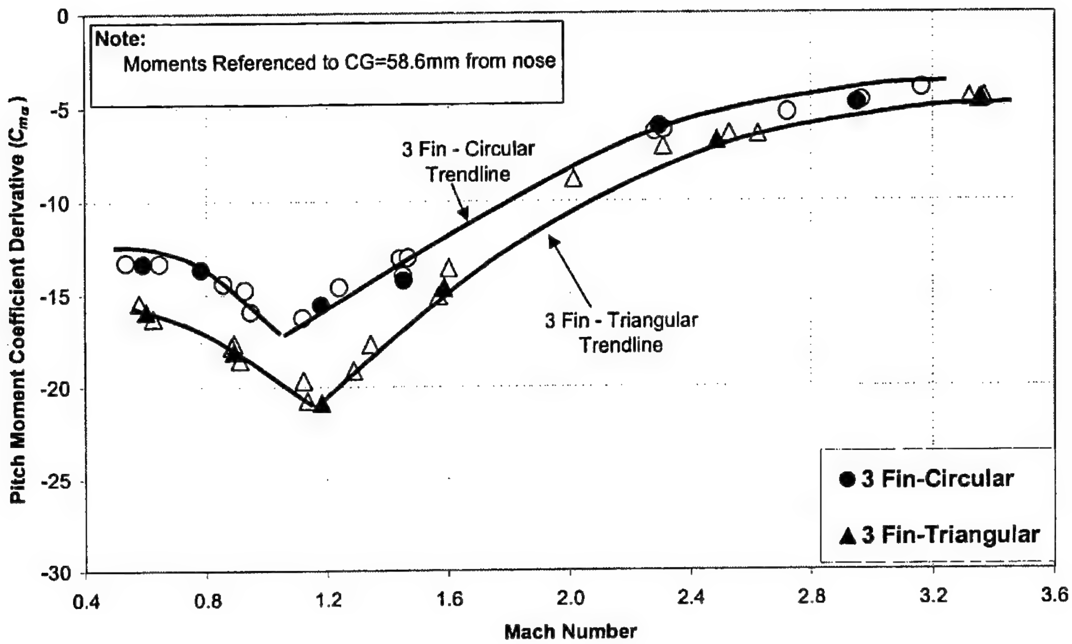

Figure 32. Pitch Moment Coefficient Derivative versus Mach Number – Triangular Cross Section Configuration

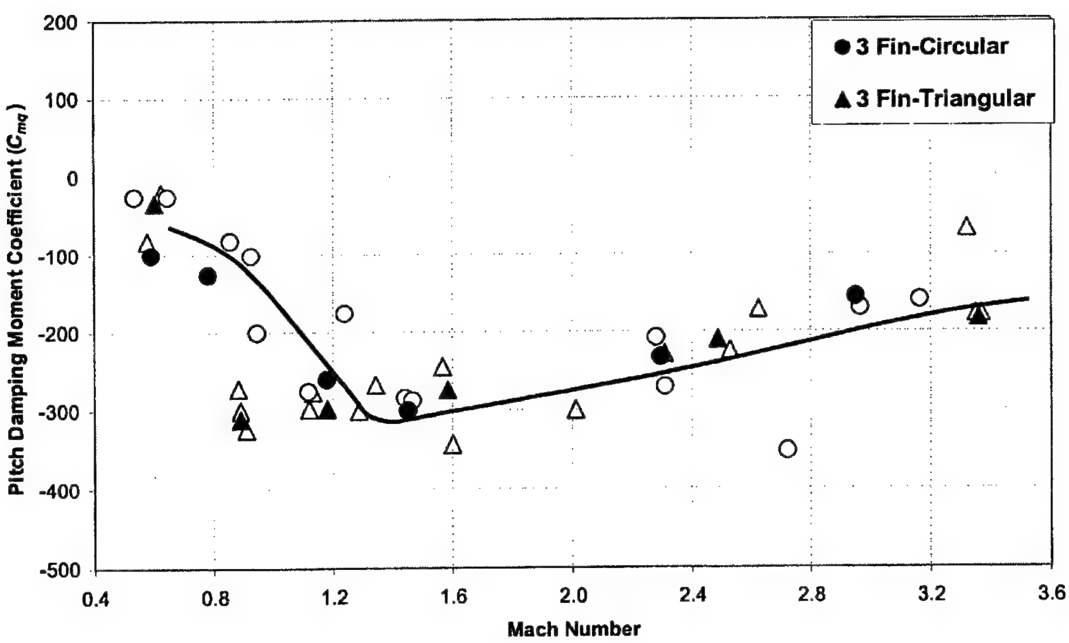

Figure 33. Pitch Damping Moment Coefficient versus Mach Number – Triangular Cross Section Configuration

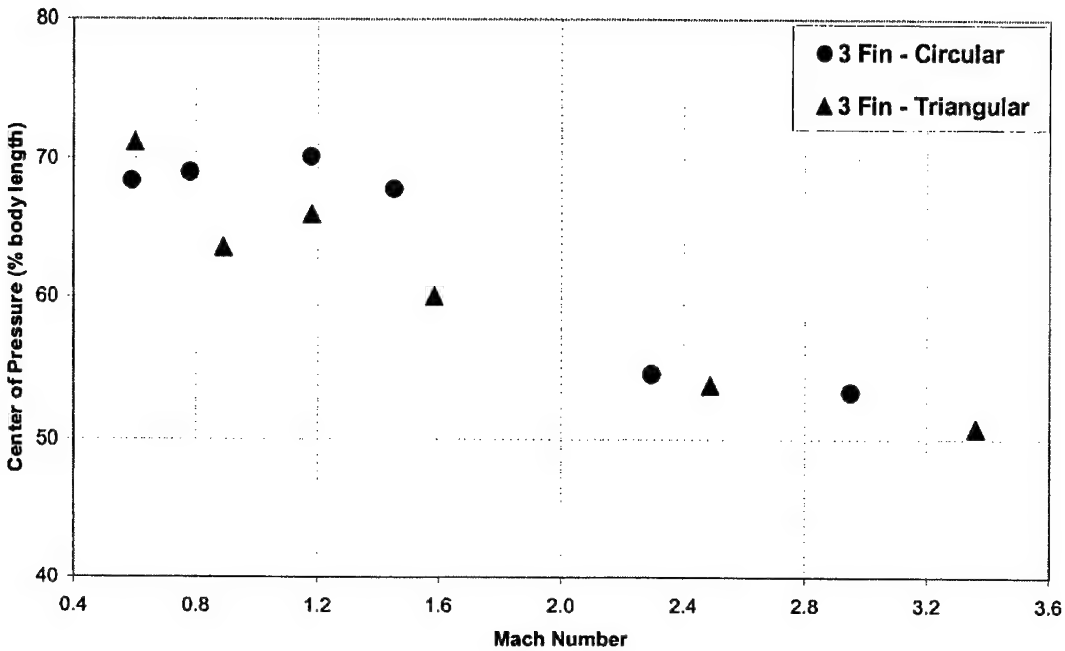

Figure 34. Center of Pressure Location versus Mach Number (enhanced scale) Triangular Cross Section Configuration

SECTION IV

CONCLUSIONS

This report documents experimental aerodynamic test results of a variety of cross sectional shapes; all of which have the same cross sectional area. Aerodynamic force and moment coefficients have been extracted from free-flight data measured in the AFRL Aeroballistic Research Facility (ARF). The range of Mach numbers covered during these trials ranged from Mach 0.75 to 3.5 and comprised a total of 104 flights. A total of seven configurations were tested and evaluated: four-fin circular, three-fin circular, 0.8 eccentric elliptical (four-fin), 0.6 eccentric elliptical (four-fin), 0.8/0.6 eccentric blended elliptical (four-fin), four-fin square, and three-fin triangular.

These experimental test results provide a good comparison of the shape effects on the basic aerodynamics with respect to axial force, normal force, and pitching moment. There is a high degree of confidence in the aerodynamic data derived from these ballistics range tests. There was repeatability and a common set of aerodynamics was derived from multiple flights.

The circular cross section configurations, a 4-fin and a 3-fin configuration, established a baseline reference of experimental aerodynamics for comparison to the non-axisymmetric configurations.

With respect to axial force, the elliptical cross sections did not exhibit any increase in drag, but did result in increased normal force. However, both the square and triangular cross section configurations incurred a drag penalty to achieve an increase in normal force.

This aeroballistic test program has provided an experimental aerodynamic database that can be used to improve aeroprediction methodologies.

Additional testing at higher angles of attack, especially for the elliptical configurations, is recommended. The test flight data reported here do not contain large enough angular motion amplitude to accurately quantify aerodynamic asymmetries.

INTENTIONALLY LEFT BLANK

APPENDIX A - NOMENCLATURE

6DOF	Six degree of freedom
AFB	Air Force Base
AFRL	Air Force Research Laboratory
AFRS	Air Force Research Shape
ARF	Aeroballistic Research Facility
ARFDAS	Aeroballistic Research Facility Data Analysis System
C	Celsius
CADRA	Comprehensive Aerodynamic Data Reduction Analysis
CG	Center of gravity
Ix	Moment of inertia about x-axis
Ixy	Cross product moment of inertia
Iy	Moment of inertia about y-axis
Iz	Moment of inertia about z-axis
M	Mach number
mbar	milibar
MLM	Maximum Likelihood Method
UF/GERC	University of Florida Graduate Engineering and Research Center
X_{CG}	Center of gravity location w.r.t nose
X_{CP}	Center of pressure location w.r.t nose

INTENTIONALLY LEFT BLANK

APPENDIX B – FIXED PLANE AERODYNAMIC MODEL

1. 6DOF - Methodology

The aerodynamic data presented in this report obtained using the "fixed plane" 6DOF analysis is detailed in this appendix. Here, the equations of motion are derived with respect to a fixed plane coordinate system. The x-axis points downrange, the y-axis points to the left looking downrange, and the z-axis points up.

FIXED PLANE EQUATIONS OF MOTION

$$\dot{u} = g\sin\theta - qw + rv - a_{cu} + F_x / \overline{m}$$
$$\dot{v} = -ru - rw\tan\theta - a_{cv} + F_y / \overline{m}$$
$$\dot{w} = -g\cos\theta + rv\tan\theta + qu - a_{cw} + F_z / \overline{m}$$
$$\dot{p} = l / I_x$$
$$\dot{q} = -r^2 \tan\theta - (I_x / I_y) rp + m / I_y$$
$$\dot{r} = qr\tan\theta + (I_x / I_y) qp + n / I_y$$

Where a_{cu}, a_{cv}, and a_{cw} are coriolis accelerations dependent on the latitude λ_R and azimuth δ_R of the range and rotational rate of the earth ω_e.

BODY FIXED CORIOLIS ACCELERATIONS

$$a_{cx} = -2\omega_e(\dot{y}\sin\lambda_R + \dot{z}\cos\lambda_R \sin\delta_R)$$
$$a_{cy} = +2\omega_e(\dot{x}\sin\lambda_R - \dot{z}\cos\lambda_R \cos\delta_R)$$
$$a_{cz} = +2\omega_e(\dot{x}\cos\lambda_R \sin\delta_R + \dot{y}\cos\lambda_R \cos\delta_R)$$
$$a_{cu} = +a_{cx}\cos\theta\cos\psi + a_{cy}\cos\theta\sin\psi - a_{cz}\sin\theta$$
$$a_{cv} = -a_{cx}\sin\psi + a_{cy}\cos\psi$$
$$a_{cw} = +a_{cx}\sin\theta\cos\psi + a_{cy}\sin\theta\sin\psi + a_{cz}\cos\theta$$

Once the aerodynamic forces and moments (i.e., F_x, F_y, F_z, l, m, n) are determined, the solution of the Equations of Motion will define the 6DOF flight motion with respect to the fixed plane coordinate system. Since the position-attitude measurements, as acquired from the ballistic spark range, are relative to the Earth-fixed coordinate system, additional transformation equations are required. These transformation equations are shown below in terms of the fixed plane Euler angles (θ, ψ) and the angle of rotation about the missile axis (ϕ).

EARTH FIXED TRANSFORMATION EQUATIONS (FIXED PLANE)

$$
\begin{aligned}
\dot{x} &= u\cos\theta\cos\psi - v\sin\psi + w\sin\theta\cos\psi \\
\dot{y} &= u\cos\theta\sin\psi + v\cos\psi + w\sin\theta\sin\psi \\
\dot{z} &= -u\sin\theta + w\cos\theta \\
\dot{\theta} &= q \\
\dot{\psi} &= r/\cos\theta \\
\dot{\phi} &= p + r\tan\theta
\end{aligned}
$$

The Equations of Motion and the Earth Fixed Transformation Equations ar numerically integrated using a fourth-order Runge-Kutta scheme.

2. Aerodynamic Forces and Moments.

The fixed plane aerodynamic forces and moments are defined as follows:

$$
\begin{aligned}
F_x &= -\overline{q}A\overline{C}_X \\
F_y &= \overline{q}A[-\overline{C}_{N\alpha}\frac{v}{V} + \frac{pd}{2V}\overline{C}_{Yp\alpha}\frac{w}{V} \\
&\quad + (\overline{C}_{N\delta}\delta_A)\sin\phi - (\overline{C}_{N\delta}\delta_B)\cos\phi] \\
F_z &= \overline{q}A[-\overline{C}_{N\alpha}\frac{w}{V} - \frac{pd}{2V}\overline{C}_{Yp\alpha}\frac{v}{V} - \overline{C}_{Y_{\varphi\alpha}}\frac{v}{V} \\
&\quad - (\overline{C}_{N\delta}\delta_A)\sin\phi - (\overline{C}_{N\delta}\delta_B)\sin\phi] \\
l &= \overline{q}A[\frac{pd}{2V}\overline{C}_{lp} + \overline{C}_l] \\
m &= \overline{q}Ad[\overline{C}_{m\alpha}\frac{w}{V} + \frac{qd}{2V}\overline{C}_{mq} + \frac{pd}{2V}\overline{C}_{np\alpha}\frac{v}{V} \\
&\quad + \overline{C}_{n\gamma\alpha}\frac{v}{V} + \overline{C}_{n\alpha}\frac{v}{V} + \overline{C}_{m\delta}\delta_A\cos\phi - \overline{C}_{m\delta}\delta_B\sin\phi] \\
n &= \overline{q}Ad[-\overline{C}_{m\alpha}\frac{v}{V} + \frac{rd}{2V}\overline{C}_{mq} + \frac{pd}{2V}\overline{C}_{np\alpha}\frac{w}{V} \\
&\quad + \overline{C}_{n\gamma\alpha}\frac{w}{V} + \overline{C}_{n\alpha}\frac{w}{V} + \overline{C}_{m\delta}\delta_A\sin\phi + \overline{C}_{m\delta}\delta_B\cos\phi]
\end{aligned}
$$

where:

A = reference area

d = reference length

$\overline{q}$ = dynamic pressure $= \frac{1}{2}\rho V^2$

$V = \sqrt{u^2 + v^2 + w^2}$

The aerodynamic coefficients and derivatives are assumed to be nonlinear functions of Mach number, sine of the total angle of attack, and the aerodynamic roll angle. This assumption is made in a general sense in defining a generalized aerodynamic math model. These expansion are shown as follows:

AERODYNAMIC COEFFICIENT EXPANSIONS (FIXED PLANE)

Axial Force Coefficient

$$\overline{C}_X = C_{XO} + C_{X\alpha_2}\varepsilon^2 + C_{X\alpha_4}\varepsilon^4 + C_{Xm}(M_i - M_r) + C_{Xm2}(M_i - M_r)^2 + C_{X\gamma\alpha_2}\varepsilon^2 \cos N$$

Normal Force Coefficient Derivative

$$\overline{C}_{N\alpha} = C_{N\alpha} + C_{N\alpha_3}\varepsilon^2 + C_{N\alpha_5}\varepsilon^4 + C_{N\alpha m}(M_i - M_r) + C_{N\gamma\alpha_3}\varepsilon^2 \cos N_\gamma$$

Magnus Force Coefficient Derivative

$$\overline{C}_{Yp\alpha} = C_{Yp\alpha} + C_{Yp\alpha_3}\varepsilon^2$$

Induced Side Force Coefficient

$$\overline{C}_{Y\gamma\alpha} = C_{Y\gamma\alpha_3}\varepsilon^2 \sin N\gamma$$

Spin Decay Roll Moment Coefficient

$$\overline{C}_{lp} = C_{lp} + C_{lp\alpha_2}\varepsilon^2 + C_{lpm}(M_i - M_r)$$

Static/Induced Roll Moment Coefficient

$$\overline{C}_l = C_{l\delta}\delta + C_{l\gamma\alpha 2} \sin N\gamma$$

Pitching Moment Coefficient Derivative

$$\overline{C}_{m\alpha} = C_{m\alpha} + C_{m\alpha_3}\varepsilon^2 + C_{m\alpha_5}\varepsilon^4 + C_{m\alpha m}(M_i - M_r) + C_{m\alpha m2}(M_i - M_r)^2$$
$$+ C_{N\alpha}(CG - CG_r) + C_{m\gamma\alpha_3}\varepsilon^2 \cos N\gamma + C_{mp\alpha}\left(\frac{pd}{2V}\right)$$

Pitch Damping Moment Coefficient

$$\overline{C}_{mq} = C_{mq} + C_{mq\alpha_2}\varepsilon^2 + C_{mq_4}\varepsilon^4 + C_{mqm}(M_i - M_r)$$

Magnus Moment Coefficient Derivative

$$\overline{C}_{np\alpha} = C_{np\alpha} + C_{np\alpha_3}\varepsilon^2 + C_{np\alpha_5}\varepsilon^4 + C_{np\alpha m}(M_i - M_r)$$

Induced Side Moment Coefficient Derivative

$$\overline{C}_{n\gamma\alpha} = C_{n\gamma\alpha} \sin N_{\gamma} + C_{n\gamma\alpha_3} \varepsilon^2 \sin N_{\gamma}$$

Trim Force Coefficients

$$\overline{C}_{N\delta}\delta_A, \overline{C}_{N\delta}\delta_B$$

Trim Moment Coefficients

$$C_{m\delta}\delta_A, C_{m\delta}\delta_B$$

Out of Plane Side Moment Due to Pitch

$$\overline{C}_{n\alpha}$$

The aerodynamic roll angle, γ, is computed by transforming the fixed plane missile velocities into the rolling body coordinate system.

$$\begin{aligned} v_b &= v\cos\phi + w\sin\phi \\ w_b &= -v\sin\phi + w\cos\phi \\ \gamma &= \tan^{-1}(v_b/w_b) \end{aligned}$$

The sine of the total angle of attack is calculated as follows:

$$\varepsilon = \sqrt{\frac{v^2 + w^2}{V}}$$

Slight variations in the center of gravity (CG) between test projectiles (models) are accounted for by assigning a reference CG location (CG_T) and making an appropriate correction to the pitching moment coefficient derivative. The pitching moment coefficient is the only coefficient of which slight changes in CG have a first order effect on the observed motion.

The full 6DOF equations of motion portion of the analysis eliminates the assumptions of Linear Theory by retaining all cross coupling terms and allowing nonlinearities both as functions of Mach number and angle of attack. In addition, the procedure within ARFDAS allows analysis of up to five test flights simultaneously. This provides improved accuracy of the extracted aerodynamics and their nonlinearities with angle of attack, roll angle, and Mach number.

APPENDIX C – BODY FIXED AERODYNAMIC MODEL

1. 6DOF – Methodology

The aerodynamic data presented in this report that were obtained using the "body fixed" 6DOF analysis is detailed in this appendix. Here, the equations of motion are derived with respect to a rotating body fixed coordinate system. The *x*-axis points down the axis of the body, the *y*-axis points out the left side of the body looking downrange, and the *z*-axis points up with respect to the body. The body fixed coordinate system is rigidly affixed to the projectile and rotates with the body about the *x*-axis. The inertial frame of reference is the earth. It is assumed the earth is fixed in space and flat. The body fixed equations of motion are given as follows where the subscript "*b*" refers to the body fixed coordinate system.

BODY FIXED EQUATIONS OF MOTION

$$\dot{u}_b = g\sin\theta - q_b w_b + r_b v_b - a_{cub} + \frac{F_{xb}}{m}$$

$$\dot{v}_b = p_b w_b - r_b u_b - g\sin\phi\cos\theta - a_{cvb} + \frac{F_{yb}}{m}$$

$$\dot{w}_b = q_b u_b - p_b v_b - g\cos\phi\cos\theta - a_{cwb} + \frac{F_{zb}}{m}$$

$$\dot{p}_b = \frac{I_y l_b + I_{xy} m_b - (I_x + I_y - I_z) I_{xy} p_b r_b + (I_{xy}^2 + I_y(I_y - I_z)) q_b r_b}{(I_x I_y - I_{xy}^2)}$$

$$\dot{q}_b = \frac{I_x m_b + I_{xy} l_b + (I_x + I_y - I_z) I_{xy} q_b r_b + (I_x(I_z - I_x) - I_{xy}^2) p_b r_b}{(I_x I_y - I_{xy}^2)}$$

$$\dot{r}_b = \frac{n_b + I_{xy}(p_b^2 - q_b^2) + (I_x - I_y) p_b q_b}{I_z}$$

Where a_{cub}, a_{cvb}, *and* a_{cwb} are coriolis accelerations dependent on the latitude λ_R and azimuth δ_R of the range and rotational rate of the earth ω_e.

BODY FIXED CORIOLIS ACCELERATIONS

$$a_{cx} = -2\omega_e(\dot{y}\sin\lambda_R + \dot{z}\cos\lambda_R\sin\delta_R)$$

$$a_{cy} = +2\omega_e(\dot{x}\sin\lambda_R - \dot{z}\cos\lambda_R\cos\delta_R)$$

$$a_{cz} = +2\omega_e(\dot{x}\cos\lambda_R\sin\delta_R + \dot{y}\cos\lambda_R\cos\delta_R)$$

$$a_{cub} = a_{cx}\cos\theta\cos\psi + a_{cy}\cos\theta\sin\psi - a_{cz}\sin\theta$$

$$a_{cvb} = a_{cx}(\sin\theta\sin\phi\cos\psi - \cos\phi\sin\psi) + a_{cy}(\sin\theta\sin\phi\sin\psi + \cos\phi\cos\psi) + a_{cz}(\sin\phi\cos\theta)$$

$$a_{cwb} = a_{cx}(\sin\theta\cos\psi\cos\phi + \sin\phi\sin\psi) + a_{cy}(\sin\theta\cos\phi\sin\psi - \sin\phi\cos\psi) + a_{cz}(\cos\phi\cos\theta)$$

Once the aerodynamic forces and moments (i.e., F_x, F_y, F_z, l, m, n) are determined, the solution of the body fixed equations of motion will define the 6DOF flight motion with respect to the body fixed coordinate system. Since the position-attitude measurements, as acquired from the ballistic spark range, are relative to the Earth-fixed coordinate system, additional transformation equations are required. These transformation equations are shown below in terms of the fixed plane Euler angles (θ, ψ) and the angle of rotation about the missile axis (ϕ).

EARTH FIXED TRANSFORMATION EQUATIONS (BODY FIXED)

The Equations of Motion and the Earth Fixed Transformation Equations are numerically integrated using a fourth-order Runge-Kutta scheme.

2. Aerodynamic Forces and Moments.

The body fixed aerodynamic forces and moments are defined as follows:

$$F_{x_b} = -\overline{q}A\overline{C}_X$$

$$F_{y_b} = \overline{q}A[-\overline{C}_{Y0} - \overline{C}_{Y\beta}\frac{v_b}{V} + \frac{p_b d}{2V}\overline{C}_{Yp\alpha}\frac{w_b}{V} + \overline{C}_{Y\gamma\alpha}\frac{w_b}{V}]$$

$$F_{z_b} = \overline{q}A[-\overline{C}_{Z0} - \overline{C}_{Z\alpha}\frac{w_b}{V} - \frac{p_b d}{2V}\overline{C}_{Yp\alpha}\frac{v_b}{V} - \overline{C}_{Y\gamma\alpha}\frac{v_b}{V}]$$

$$l_b = \overline{q}A[\frac{p_b d}{2V}\overline{C}_{\ell p} + C_{\ell\delta}\delta + \overline{C}_{\ell\gamma\alpha}]$$

$$m_b = \overline{q}Ad[C_{m0} + \overline{C}_{m\alpha}\frac{w_b}{V} + \frac{q_b d}{2V}\overline{C}_{mq} + \frac{p_b d}{2V}\overline{C}_{np\alpha}\frac{v_b}{V} + \overline{C}_{n\gamma\alpha}\frac{v_b}{V}]$$

$$n_b = \overline{q}Ad[-C_{n0} - \overline{C}_{n\beta}\frac{v_b}{V} + \frac{r_b d}{2V}\overline{C}_{nr} + \frac{p_b d}{2V}\overline{C}_{np\alpha}\frac{w_b}{V} + \overline{C}_{n\gamma\alpha}\frac{w_b}{V}]$$

where:

A = reference area

d = reference length

$\overline{q}$ = dynamic pressure = $\frac{1}{2}\rho V^2$

$V = \sqrt{u_b^2 + v_b^2 + w_b^2}$

The aerodynamic coefficients and derivatives are assumed to be nonlinear functions of Mach number, sine of the total angle of attack, and the aerodynamic roll angle. This assumption is made in a general sense in defining a generalized aerodynamic math model. These expansion for the body fixed equations of motion are shown as follows:

AERODYNAMIC COEFFICIENT EXPANSIONS (BODY FIXED)

Axial Force Coefficient

$$\overline{C}_X = C_{XO} + C_{X\alpha_2}(\frac{w_b}{V})^2 + C_{X\beta_2}(\frac{v_b}{V})^2 + C_{Xm}(M_i - M_r) + C_{X\gamma\alpha_2}\varepsilon^2\cos N\gamma$$

Normal Force Coefficient Derivative

$$\overline{C}_{Z\alpha} = C_{Z\alpha} + C_{Z\alpha_3}(\frac{w_b}{V})^2 + C_{N\gamma\alpha_3}\varepsilon^2\cos N_\gamma$$

Side Force Coefficient Derivative

$$\overline{C}_{Y\beta} = C_{Y\beta} + C_{Y\beta_3}(\frac{v_b}{V})^2 + C_{N\gamma\alpha_3}\varepsilon^2 \cos N\gamma$$

Magnus Force Coefficient Derivative

$$\overline{C}_{Yp\alpha} = C_{Yp\alpha}$$

Induced Side Force Coefficient

$$\overline{C}_{Y\gamma\alpha} = C_{Y\gamma\alpha_3}\varepsilon^2 \sin N\gamma$$

Spin Decay Roll Moment Coefficient

$$\overline{C}_{\ell p} = C_{\ell p} + C_{\ell p\alpha_2}\varepsilon^2 + C_{\ell pm}(M_i - M_r)$$

Static/Induced Roll Moment Coefficient

$$\overline{C}_{\ell} = C_{\ell\delta}\delta + C_{\ell\gamma\alpha_2} \sin N\gamma$$

Pitching Moment Coefficient Derivative

$$\overline{C}_{m\alpha} = C_{m\alpha} + C_{m\alpha_3}(\frac{w_b}{V})^2 + C_{Z\alpha}(CG - CG_r) + C_{m\gamma\alpha_3}\varepsilon^2 \cos N\gamma$$

Yawing Moment Coefficient Derivative

$$\overline{C}_{n\beta} = C_{n\beta} + C_{n\beta_3}(\frac{v_b}{V})^2 + C_{Y\beta}(CG - CG_r) + C_{m\gamma\alpha_3}\varepsilon^2 \cos N\gamma$$

Pitch Damping Moment Coefficient

$$\overline{C}_{mq} = C_{mq} + C_{mq\alpha_2}(\frac{w_b}{V})^2$$

Yaw Damping Moment Coefficient

$$\overline{C}_{nr} = C_{nr} + C_{nr\alpha_2}(\frac{v_b}{V})^2$$

Magnus Moment Coefficient Derivative

$$\overline{C}_{np\alpha} = C_{np\alpha}$$

Induced Side Moment Coefficient Derivative

$$\overline{C}_{n\gamma\alpha} = C_{n\gamma\alpha_3}\varepsilon^2 \sin N_\gamma + C_{n\gamma\alpha_5}\varepsilon^4 \sin N_\gamma$$

Trim Force Coefficients

$$\overline{C}_{Z0},\ \overline{C}_{Y0}$$

Trim Moment Coefficients

$$\overline{C}_{m0},\ \overline{C}_{n0}$$

The aerodynamic roll angle, γ, is computed as follows:

$$\gamma = \tan^{-1}(v_b / w_b)$$

The sine of the total angle of attack is calculated as follows:

$$\varepsilon = \sqrt{\frac{v^2 + w^2}{V}}$$

The body fixed pitch and yaw angles are defined as follows:

$$\alpha = \frac{w_b}{V}$$

$$\beta = \frac{v_b}{V}$$

Slight variations in the center of gravity (CG) between test projectiles (models) are accounted for by assigning a reference CG location (CG_r) and making an appropriate correction to the pitching moment coefficient derivative. The pitching moment coefficient is the only coefficient of which slight changes in CG have a first order effect on the observed motion.

The full 6DOF equations of motion portion of the analysis eliminates the assumptions of Linear Theory by retaining all cross coupling terms and allowing nonlinearities both as functions of Mach number and angle of attack. In addition, the procedure within ARFDAS allows analysis of up to five test flights simultaneously. This provides improved accuracy of the extracted aerodynamics and their nonlinearities with angle of attack, roll angle, and Mach number.

INTENTIONALLY LEFT BLANK

APPENDIX D –FLIGHT TRIAL DATA

1. Four-Fin Circular

Table D-1: 4-Fin Circular Model Physical Properties

Shot Number	Projectile Diameter (mm)	Mass (kg)	Axial Inertia (kg- m2)	Inertia Y (kg- m2)	Inertia Z (kg- m2)	Inertia XY (kg- m2)	Length (mm)	CG (mm from nose)	Spin
S971027	17.000	.843E-01	.360E-05	.127E-03	.127E-03	.000	137.500	58.634	Yes
S971032	17.000	.844E-01	.360E-05	.127E-03	.127E-03	.000	137.500	58.986	Yes
S971037	17.000	.844E-01	.360E-05	.127E-03	.127E-03	.000	137.500	58.986	Yes
S980944	17.000	.843E-01	.360E-05	.127E-03	.127E-03	.000	137.500	58.724	Yes
S971038	17.000	.845E-01	.358E-05	.127E-03	.127E-03	.000	137.500	58.131	Yes
S971033	17.000	.845E-01	.360E-05	.127E-03	.127E-03	.000	137.500	58.916	Yes
S971022	17.000	.846E-01	.365E-05	.127E-03	.127E-03	.000	137.500	58.846	Yes
S971024	17.000	.843E-01	.360E-05	.127E-03	.127E-03	.000	137.500	58.634	Yes
S971039	17.000	.844E-01	.360E-05	.127E-03	.127E-03	.000	137.500	58.986	Yes
S980258	17.000	.843E-01	.360E-05	.127E-03	.127E-03	.000	137.500	58.724	Yes
S980253	17.000	.843E-01	.360E-05	.127E-03	.127E-03	.000	137.500	58.724	Yes
S980254	17.000	.843E-01	.360E-05	.127E-03	.127E-03	.000	137.500	58.724	Yes
S990523	17.000	.843E-01	.360E-05	.127E-03	.127E-03	.000	137.500	58.724	Yes
S000566	17.000	.843E-01	.360E-05	.127E-03	.127E-03	.000	137.500	58.724	Yes
S990522	17.000	.843E-01	.360E-05	.127E-03	.127E-03	.000	137.500	58.724	Yes

Table D-2: 4-Fin Circular Range Conditions

Shot Number	No. of Stations	Observed Distance (m)	Pressure (mbar)	Temperature (degrees C)	Relative Humidity %	Air Density (kg/m3)	Speed of Sound (m/sec)	Reynolds Number (x10**-7)
S971027	10	36.6	1024.05000	21.60	51.0000	1.2103	344.169	.173
S971032	13	54.9	1021.00000	20.49	53.0000	1.2113	343.521	.230
S971037	17	71.6	1021.00000	20.49	53.0000	1.2113	343.521	.245
S980944	28	105.2	1015.92000	20.28	54.0000	1.2061	343.398	.249
S971038	22	74.7	1021.00000	20.49	53.0000	1.2113	343.521	.283
S971033	19	74.7	1015.92000	20.97	51.0000	1.2033	343.801	.307
S971022	21	82.3	1022.01000	21.25	59.0000	1.2094	343.965	.447
S971024	24	82.3	1019.98000	21.11	56.0000	1.2075	343.883	.452
S971039	22	74.7	1019.30000	20.56	54.0000	1.2090	343.561	.461
S980258	47	199.7	1010.84000	20.69	53.0000	1.1984	343.637	.701
S980253	45	199.6	982.73000	20.49	50.0000	1.1659	343.521	.691
S980254	45	199.7	1016.60000	21.60	53.0000	1.2015	344.169	.731
S990523	39	179.9	1014.90000	20.21	57.0000	1.2052	343.357	.964
S000566	45	190.5	1015.92000	20.56	61.0000	1.2050	343.561	1.001
S990522	32	160.1	1020.32000	20.49	56.0000	1.2105	343.521	1.077

Table D-3: 4-Fin Circular 6DOF Aerodynamics – Single Fits

Shot Number	Mach Number	DBSQ ABARM	CX CX2	CNa CNa3	CYpa Cnpa	Cma Cma3	Cmq Cmq2	CZga3 Cmga3	CYga3 Cnga3	Clga2 Cnsm	Clp Cld	CNda CNdB	Cmda CmdB	Standard Error X(m) Y-Z(m)	Angle(deg) Roll(deg)
S971027	.551	.5	.301	7.85	.00	-17.462	-26.0	.0	.0	.00	-3.000	.004	.005	.0012	.315
		.8	3.30	.0	.0	.0	.0	.0	.0	.00	.001	-.009	-.034	.0004	3.341
S971032	.731	1.2	.316	8.00	.00	-18.424	-26.0	.0	.0	.00	-3.000	-.010	.020	.0019	.252
		1.6	3.61	.0	.0	.0	.0	.0	.0	.00	.001	.015	.056	.0004	1.419
S971037	.778	3.5	.333	8.10	.00	-17.812	-26.0	.0	.0	.00	-3.000	-.012	.031	.0014	.220
		3.2	3.73	.0	.0	.0	.0	.0	.0	.00	-.002	.007	-.009	.0013	3.056
S980944	.792	3.1	.292	8.30	.00	-17.973	-26.0	.0	.0	.00	-4.532	-.008	.035	.0019	.343
		3.0	3.76	.0	.0	.0	.0	.0	.0	.00	-.007	.024	.082	.0007	4.495
S971038	.900	.5	.342	8.50	.00	-18.506	-125.0	.0	.0	.00	-3.000	-.005	.012	.0011	.183
		1.6	4.23	.0	.0	.0	.0	.0	.0	.00	.001	.007	.030	.0012	2.500
S971033	.982	.3	.432	8.50	.00	-24.322	-125.0	.0	.0	.00	-3.000	.000	.027	.0014	.257
		1.1	5.07	.0	.0	.0	.0	.0	.0	.00	.001	.000	-.008	.0003	1.818
S971022	1.423	1.1	.584	9.80	.00	-18.165	-283.6	.0	.0	.00	-3.000	.033	-.063	.0014	.178
		2.2	6.77	.0	.0	.0	.0	.0	.0	.00	.000	.002	.004	.0007	6.759
S971024	1.442	.3	.579	9.80	.00	-17.685	-262.0	.0	.0	.00	-3.000	-.015	.032	.0009	.120
		1.6	6.70	.0	.0	.0	.0	.0	.0	.00	.001	.005	.011	.0007	5.832
S971039	1.466	.1	.575	9.80	.00	-17.838	-300.0	.0	.0	.00	-3.000	.018	-.027	.0015	.187
		.8	6.60	.0	.0	.0	.0	.0	.0	.00	.004	-.023	-.062	.0008	3.280
S980258	2.251	3.1	.486	7.37	.00	-10.929	-233.7	.0	.0	.00	-3.000	.011	-.018	.0015	.146
		4.9	4.96	.0	.0	.0	.0	.0	.0	.00	-.005	-.001	-.008	.0005	14.080
S980253	2.279	.4	.510	7.67	.00	-10.664	-232.8	.0	.0	.00	-3.000	-.003	.002	.0014	.157
		2.0	4.94	.0	.0	.0	.0	.0	.0	.00	-.002	.003	.011	.0005	6.981
S980254	2.343	.3	.486	6.63	.00	-10.267	-197.3	.0	.0	.00	-3.000	.011	-.028	.0010	.125
		1.6	4.86	.0	.0	.0	.0	.0	.0	.00	-.002	-.001	-.012	.0004	5.930
S990523	3.075	.5	.414	5.95	.00	-7.377	-203.7	.0	.0	.00	-1.156	-.002	-.005	.0013	.154
		2.2	3.78	.0	.0	.0	.0	.0	.0	.00	.000	.012	.027	.0007	9.130
S000566	3.195	.3	.413	5.80	.00	-6.790	-139.6	.0	.0	.00	-4.318	.008	-.022	.0015	.167
		1.5	3.71	.0	.0	.0	.0	.0	.0	.00	-.003	.011	.028	.0005	4.704
S990522	3.422	1.1	.391	5.20	.00	-6.125	-188.2	.0	.0	.00	-.191	.003	.005	.0016	.165
		2.4	3.58	.0	.0	.0	.0	.0	.0	.00	-.003	-.006	-.020	.0007	9.315

Table D-4: 4-Fin Circular 6DOF Aerodynamics – Multiple Fits

Shot Numbers		Mach Number	DBSQ ABARM	CX CX2 CX4	CNa CNa3 CNa5	CYpa Cnpa Cnpa3	Cma Cma3 Cma5	Cmq Cmq2 Cmq4	CZga3 Cmga3 Cmga	CYga3 Cnga3 Cnga5	Clga2 CXga2 Clp	CXM CmaM CnsM	Standard Error X(m) Y-Z(m)	Standard Error Angle(deg) Roll(deg)
S971027	S971032	.641	.9	.309	7.85	.00	-18.376	-26.0	.0	.0	.00	.09	.0016	.284
			1.5	3.61	.0	.00	.0	.0	.0	.0	.00	.00	.0004	2.334
				.0	.0	.0	.0	.0	.0	.0	-3.00	.00		
S971027	S971032	.713	2.0	.301	7.97	.00	-17.959	-26.0	.0	.0	.00	.22	.0017	.296
S971037	S980944		3.2	3.50	.0	.00	.0	.0	.0	.0	.00	.00	.0008	3.581
				.0	.0	.0	.0	.0	.0	.0	-4.53	.00		
S980944	S971037	.785	3.2	.313	7.80	.00	-17.920	-22.1	.0	.0	.00	-.20	.0018	.312
			3.1	3.73	.0	.00	.0	.0	.0	.0	.00	.00	.0010	4.238
				.0	.0	.0	.0	.0	.0	.0	-3.00	.00		
S971033	S971038	.941	.4	.379	8.50	.00	-21.252	-156.1	.0	.0	.00	1.18	.0013	.221
			1.5	4.23	.0	.00	.0	.0	.0	.0	.00	-67.99	.0009	2.377
				.0	.0	.0	.0	.0	.0	.0	-3.00	.00		
S971039	S971024	1.444	.5	.579	9.84	.00	-18.081	-281.4	.0	.0	.00	-.23	.0015	.188
S971022			2.1	6.77	.0	.00	.0	.0	.0	.0	.02	.00	.0007	4.748
				.0	.0	.0	.0	.0	.0	.0	-3.00	.00		
S980253	S980254	2.291	1.2	.486	7.15	.00	-10.895	-235.8	.0	.0	.00	-.16	.0013	.157
S980258			4.9	4.96	.0	.00	.0	.0	.0	.0	.01	3.85	.0006	9.983
				.0	.0	.0	.0	.0	.0	.0	-3.00	.00		
S990523	S000566	3.231	.6	.411	5.80	.00	-6.890	-178.8	.0	.0	.00	-.07	.0014	.161
S990522			2.4	3.58	.0	.00	.0	.0	.0	.0	.00	3.37	.0007	8.073
				.0	.0	.0	.0	.0	.0	.0	-3.09	.00		

2. Three-Fin Circular

Table D-5: 3-Fin Circular Model Physical Properties

Shot Number	Projectile Diameter (mm)	Mass (kg)	Axial Inertia (kg- m2)	Inertia Y (kg- m2)	Inertia Z (kg- m2)	Inertia XY (kg- m2)	Length (mm)	CG (mm from nose)	Spin
S971035	17.000	.835E-01	.346E-05	.123E-03	.123E-03	.000	137.500	58.131	Yes
S971028	17.000	.835E-01	.346E-05	.123E-03	.123E-03	.000	137.500	58.025	Yes
S971031	17.000	.835E-01	.346E-05	.123E-03	.123E-03	.000	137.500	57.992	Yes
S971030	17.000	.835E-01	.346E-05	.123E-03	.123E-03	.000	137.500	58.061	Yes
S971036	17.000	.835E-01	.346E-05	.123E-03	.123E-03	.000	137.500	58.131	Yes
S971034	17.000	.835E-01	.346E-05	.123E-03	.123E-03	.000	137.500	58.061	Yes
S971040	17.000	.835E-01	.346E-05	.123E-03	.123E-03	.000	137.500	58.061	Yes
S980252	17.000	.835E-01	.346E-05	.123E-03	.123E-03	.000	137.500	58.060	Yes
S971021	17.000	.835E-01	.346E-05	.123E-03	.123E-03	.000	137.500	58.062	Yes
S971023	17.000	.835E-01	.346E-05	.123E-03	.123E-03	.000	137.500	58.065	Yes
S980255	17.000	.835E-01	.346E-05	.123E-03	.123E-03	.000	137.500	58.606	Yes
S980256	17.000	.835E-01	.346E-05	.123E-03	.123E-03	.000	137.500	58.606	Yes
S990524	17.000	.835E-01	.346E-05	.123E-03	.123E-03	.000	137.500	58.060	Yes
S990525	17.000	.835E-01	.346E-05	.123E-03	.123E-03	.000	137.500	58.060	Yes
S000567	17.000	.835E-01	.346E-05	.123E-03	.123E-03	.000	137.500	58.606	Yes

Table D-6: 3-Fin Circular Range Conditions

Shot Number	No. of Stations	Observed Distance (m)	Pressure (mbar)	Temperature (degrees C)	Relative Humidity %	Air Density (kg/m3)	Speed of Sound (m/sec)	Reynolds Number (x10**-7)
S971035	10	36.6	1021.00000	20.49	53.0000	1.2113	343.521	.168
S971028	13	50.3	1024.05000	21.60	51.0000	1.2103	344.169	.203
S971031	15	54.9	1015.92000	20.97	51.0000	1.2033	343.801	.267
S971030	18	62.4	1024.05000	21.06	51.0000	1.2126	343.854	.292
S971036	21	74.7	1021.00000	20.49	53.0000	1.2113	343.521	.298
S971034	22	74.7	1015.92000	21.06	51.0000	1.2029	343.855	.349
S971040	23	74.7	1019.30000	20.56	54.0000	1.2090	343.561	.291
S980252	44	199.7	982.73000	20.49	50.0000	1.1659	343.521	.437
S971021	24	82.3	1022.01000	21.25	59.0000	1.2094	343.965	.456
S971023	24	80.7	1019.98000	21.11	56.0000	1.2075	343.883	.461
S980255	45	198.1	1016.60000	21.60	53.0000	1.2015	344.169	.711
S980256	45	199.7	1014.90000	20.83	54.0000	1.2027	343.719	.722
S990524	42	199.7	1014.90000	20.21	57.0000	1.2052	343.357	.853
S990525	39	199.6	1021.34000	20.62	57.0000	1.2112	343.597	.934
S000567	47	195.2	1015.92000	20.56	61.0000	1.2050	343.561	.991

Table D-7: 3-Fin Circular 6DOF Aerodynamics – Single Fits

Shot Number	Mach Number	DBSQ ABARM	CX CX2	CNa CNa3	CYpa Cnpa	Cma Cma3	Cmq Cmq2	CZga3 Cmga3	CYga3 Cnga3	Clga2 Cnsm	Clp Cld	CNda CNdB	Cmda CmdB	Standard Error X(m) Y-Z(m)	Standard Error Angle(deg) Roll(deg)
S971035	.534	3.7 3.0	.282 3.30	6.20 .0	.00 .0	-13.281 .0	-25.0 .0	.0 .0	.0 .0	.00 .00	-3.000 -.001	-.012 .006	.026 -.037	.0025 .0006	.108 2.903
S971028	.645	2.0 2.3	.300 3.41	6.15 .0	.00 .0	-13.339 .0	-25.0 .0	.0 .0	.0 .0	.00 .00	-3.671 .002	.005 .009	-.014 .035	.0014 .0004	.141 4.774
S971031	.855	2.9 3.0	.303 4.04	6.50 .0	.00 .0	-14.408 .0	-81.9 .0	.0 .0	.0 .0	.00 .00	-2.064 .005	.000 .000	.001 -.029	.0011 .0004	.199 2.410
S971030	.926	2.4 3.0	.331 4.49	6.80 .0	.00 .0	-14.758 .0	-101.1 .0	.0 .0	.0 .0	.00 .00	-2.120 .000	.000 .000	.006 .000	.0010 .0004	.163 2.254
S971036	.946	2.3 3.7	.345 4.68	6.80 .0	.00 .0	-15.942 .0	-200.3 .0	.0 .0	.0 .0	.00 .00	-2.136 -.001	.000 .000	.016 -.003	.0012 .0011	.140 4.897
S971034	1.118	.8 2.2	.552 6.98	7.00 .0	.00 .0	-16.275 .0	-275.2 .0	.0 .0	.0 .0	.00 .00	-2.298 .001	-.007 -.007	.034 -.014	.0010 .0007	.073 2.581
S971040	1.240	.1 .6	.569 7.54	7.00 .0	.00 .0	-14.634 .0	-175.6 .0	.0 .0	.0 .0	.00 .00	-2.304 -.007	-.001 .017	-.008 .020	.0016 .0006	.080 3.493
S980252	1.442	.6 3.7	.556 6.71	7.30 .0	.00 .0	-13.089 .0	-283.9 .0	.0 .0	.0 .0	.00 .00	-2.159 .001	.006 .003	-.009 .011	.0019 .0021	.102 13.360
S971021	1.452	.0 .5	.539 6.66	7.00 .0	.00 .0	-13.998 .0	-300.0 .0	.0 .0	.0 .0	.00 .00	-2.153 -.001	.000 .000	-.018 -.029	.0017 .0005	.116 5.146
S971023	1.468	.4 1.2	.534 6.59	7.00 .0	.00 .0	-13.032 .0	-287.2 .0	.0 .0	.0 .0	.00 .00	-2.145 -.001	-.004 .006	.010 .015	.0011 .0005	.107 5.150
S980255	2.280	.2 1.8	.456 4.82	6.97 .0	.00 .0	-6.288 .0	-208.2 .0	.0 .0	.0 .0	.00 .00	-3.829 -.004	-.007 .000	.011 .004	.0015 .0008	.089 5.442
S980256	2.310	2.0 6.2	.449 4.79	6.18 .0	.00 .0	-6.193 .0	-270.7 .0	.0 .0	.0 .0	.00 .00	-3.500 -.005	-.001 -.010	.022 -.038	.0016 .0011	.250 9.692
S990524	2.723	2.1 2.8	.433 4.20	6.43 .0	.00 .0	-5.296 .0	-351.9 .0	.0 .0	.0 .0	.00 .00	-4.016 -.013	.005 -.013	-.036 -.021	.0018 .0008	.278 14.790
S990525	2.966	2.0 3.3	.415 3.85	5.85 .0	.00 .0	-4.659 .0	-169.6 .0	.0 .0	.0 .0	.00 .00	-5.382 -.023	.005 -.023	-.037 -.002	.0016 .0006	.142 8.807
S000567	3.164	.7 2.7	.395 3.69	5.25 .0	.00 .0	-4.023 .0	-159.2 .0	.0 .0	.0 .0	.00 .00	-4.239 .003	.005 .000	.001 .005	.0010 .0008	.167 3.439

Table D-8: 3-Fin Circular 6DOF Aerodynamics – Multiple Fits

Shot Numbers		Mach Number	DBSQ ABARM	CX CX2 CX4	CNa CNa3 CNa5	CYpa Cnpa Cnpa3	Cma Cma3 Cma5	Cmq Cmq2 Cmq4	CZga3 Cmga3 Cmga	CYga3 Cnga3 Cnga5	Clga2 CXga2 Clp	CXM CmaM CnsM	Standard Error X(m) Y-Z(m)	Standard Error Angle(deg) Roll(deg)
S971035	S971028	.590	2.7	.292	6.40	.00	-13.353	-100.0	.0	.0	.00	.16	.0018	.150
			3.1	3.41	.0	.00	.0	.0	.0	.0	.00	.00	.0005	3.993
				.0	.0	.0	.0	.0	.0	.0	-3.76	.00		
S971036	S971030	.781	2.6	.314	6.40	.00	-13.655	-125.6	.0	.0	.00	.16	.0029	.264
S971031	S971028		3.6	3.30	.0	.00	.0	.0	.0	.0	.00	-5.92	.0007	3.623
S971035				.0	.0	.0	.0	.0	.0	.0	-1.89	.00		
S971034	S971040	1.179	.4	.560	7.00	.00	-15.579	-260.3	.0	.0	.00	.14	.0015	.080
			2.2	7.54	.0	.00	.0	.0	.0	.0	.00	12.03	.0007	3.044
				.0	.0	.0	.0	.0	.0	.0	-2.30	.00		
S971021	S971023	1.454	.3	.553	7.00	.00	-14.262	-299.7	.0	.0	.00	-.15	.0017	.162
S980252			3.6	6.71	.0	.00	.0	.0	.0	.0	.00	17.15	.0017	9.982
				.0	.0	.0	.0	.0	.0	.0	-2.16	.00		
S980255	S980256	2.295	1.2	.453	6.20	.00	-5.998	-232.8	.0	.0	.00	-.11	.0017	.217
			6.2	4.79	.0	.00	.0	.0	.0	.0	.00	.00	.0010	7.875
				.0	.0	.0	.0	.0	.0	.0	-3.50	.00		
S000567	S990524	2.951	1.5	.415	5.54	.00	-4.792	-155.1	.0	.0	.00	-.09	.0018	.253
S990525			3.2	3.85	.0	.00	.0	.0	.0	.0	.00	2.33	.0009	10.950
				.0	.0	.0	.0	.0	.0	.0	-4.72	.00		

3. 0.8 Elliptical

Table D-9: 0.8 Elliptical Model Physical Properties

Shot Number	Projectile Diameter (mm)	Mass (kg)	Axial Inertia (kg- m2)	Inertia Y (kg- m2)	Inertia Z (kg- m2)	Inertia XY (kg- m2)	Length (mm)	CG (mm from nose)	Spin
S980925	17.000	.864E-01	.370E-05	.134E-03	.133E-03	.000	137.400	62.353	Yes
S980927	17.000	.879E-01	.391E-05	.136E-03	.136E-03	.000	137.400	62.500	Yes
S980926	17.000	.888E-01	.383E-05	.137E-03	.137E-03	.000	137.400	62.355	Yes
S980928	17.000	.908E-01	.388E-05	.134E-03	.134E-03	.000	137.400	61.680	Yes
S980934	17.000	.880E-01	.380E-05	.137E-03	.137E-03	.000	137.400	62.634	Yes
S980938	17.000	.877E-01	.380E-05	.136E-03	.135E-03	.000	137.400	62.646	Yes
S980935	17.000	.910E-01	.391E-05	.136E-03	.135E-03	.000	137.400	61.471	Yes
S980940	17.000	.881E-01	.380E-05	.136E-03	.135E-03	.000	137.400	62.361	Yes
S980942	17.000	.880E-01	.380E-05	.136E-03	.135E-03	.000	137.400	62.432	Yes
S980259	17.000	.875E-01	.378E-05	.135E-03	.135E-03	.000	137.400	61.976	Yes
S000453	17.000	.883E-01	.380E-05	.136E-03	.135E-03	.000	137.400	62.503	Yes
S971020	17.000	.882E-01	.384E-05	.137E-03	.137E-03	.000	137.400	62.874	Yes
S000452	17.000	.883E-01	.380E-05	.136E-03	.135E-03	.000	137.400	62.623	Yes
S980257	17.000	.887E-01	.375E-05	.136E-03	.136E-03	.000	137.400	62.340	Yes
S000560	17.000	.889E-01	.380E-05	.136E-03	.135E-03	.000	137.400	63.000	Yes
S000561	17.000	.879E-01	.380E-05	.136E-03	.135E-03	.000	137.400	62.705	Yes
S000557	17.000	.889E-01	.380E-05	.136E-03	.135E-03	.000	137.400	63.000	Yes

Table D-10: 0.8 Elliptical Range Conditions

Shot Number	No. of Stations	Observed Distance (m)	Pressure (mbar)	Temperature (degrees C)	Relative Humidity %	Air Density (kg/m3)	Speed of Sound (m/sec)	Reynolds Number (x10**-7)
S980925	12	44.2	1007.11000	21.04	58.0000	1.1926	343.842	.133
S980927	22	77.7	1015.58000	20.83	56.0000	1.2035	343.719	.187
S980926	22	80.8	1008.13000	21.02	54.0000	1.1939	343.830	.211
S980928	24	80.8	1015.58000	20.83	56.0000	1.2035	343.719	.215
S980934	28	105.2	1015.92000	20.97	57.0000	1.2033	343.801	.250
S980938	29	100.6	1017.27000	21.46	56.0000	1.2029	344.087	.280
S980935	28	100.6	1016.26000	20.34	54.0000	1.2063	343.433	.305
S980940	39	181.4	1016.26000	20.97	54.0000	1.2037	343.801	.389
S980942	44	181.4	1016.26000	20.90	56.0000	1.2040	343.760	.427
S980259	43	199.7	1010.84000	20.69	53.0000	1.1984	343.637	.429
S000453	47	199.7	1017.27000	19.51	54.0000	1.2109	342.947	.588
S971020	31	140.1	1019.30000	21.18	58.0000	1.2064	343.924	.620
S000452	44	199.7	1017.27000	19.51	54.0000	1.2109	342.947	.666
S980257	44	199.7	1014.90000	20.83	54.0000	1.2027	343.719	.715
S000560	40	199.6	1017.27000	19.72	59.0000	1.2100	343.070	1.016
S000561	44	199.7	1017.27000	19.72	59.0000	1.2100	343.070	1.045
S000557	45	199.6	1021.34000	19.31	58.0000	1.2166	342.830	1.120

Table D-11: 0.8 Elliptical 6DOF Aerodynamics – Single Fits

Shot Number	Mach Number	DBSQ	CX	CYB	CZA	CY0	CnB	Cma	Cn0	Cnr	Cmq	CXaB2	Clp	Standard Error X(m)	Standard Error Angle(deg)
		ABARM	CXA2	CYB3	CZA2	CZ0	CnB3	Cma3	Cm0	Cnr2	Cmq2	CmaB3	Cld	Y-Z(m)	Roll(deg)
S980925	.429	3.5	.328	8.00	10.00	.0000	-14.87	-14.51	.0000	-100.	-124.	3.300	-1.9	.0018	.331
		3.3	.000	.0	.0	.0000	.0	.0	.0000	0.	0.	.0	.003	.0007	3.269
S980927	.597	3.0	.285	8.00	10.00	.0000	-16.21	-14.94	.1069	-151.	-239.	3.300	-6.0	.0019	.283
		2.7	.000	.0	.0	.0000	.0	.0	-.0439	0.	0.	.0	.043	.0008	2.461
S980926	.680	3.4	.291	7.79	10.37	-.0027	-15.67	-15.15	.0041	145.	-433.	3.491	-1.9	.0017	.250
		2.7	.000	.0	.0	-.0073	.0	.0	.0168	0.	0.	.0	.003	.0006	3.649
S980928	.687	.8	.316	8.00	10.00	-.0134	-14.36	-15.57	-.0450	238.	-538.	.500	-6.0	.0012	.217
		1.4	.000	.0	.0	.0474	.0	.0	-.0850	0.	0.	.0	-.001	.0008	2.565
S980934	.799	8.6	.365	8.81	11.40	.1745	-14.87	-19.92	.4647	-111.	-330.	3.500	-18.0	.0017	.220
		5.7	.000	.0	.0	-.0060	.0	.0	.0210	0.	0.	.0	.012	.0007	5.901
S980938	.896	2.6	.331	10.00	12.00	-.0377	-15.64	-18.41	-.0797	-100.	-314.	4.227	-2.1	.0017	.308
		4.2	.000	.0	.0	.0242	.0	.0	-.0413	0.	0.	.0	.003	.0013	3.331
S980935	.973	1.2	.395	10.01	15.71	.0000	-20.05	-24.16	-.0078	-121.	-315.	4.940	-2.1	.0009	.168
		2.6	.000	.0	.0	.0000	.0	.0	.0047	-68.	-39.	.0	.002	.0005	1.892
S980940	1.244	1.2	.607	8.00	10.91	-.0019	-14.81	-16.74	-.0060	-221.	-252.	.500	-4.5	.0016	.183
		2.5	.000	.0	.0	.0446	.0	.0	-.0805	0.	0.	.0	.005	.0006	5.459
S980942	1.365	1.8	.593	8.07	10.39	.0014	-14.88	-16.05	-.0041	-252.	-218.	.500	-4.9	.0017	.227
		3.1	.000	.0	.0	.0273	.0	.0	-.0625	0.	0.	.0	.007	.0005	6.212
S980259	1.379	.7	.588	9.02	8.98	-.0027	-16.01	-13.84	-.0024	-97.	-376.	.500	-4.5	.0013	.118
		2.2	.000	.0	.0	.0297	.0	.0	-.0436	0.	0.	.0	.006	.0005	2.875
S000453	1.868	1.6	.526	7.00	8.79	.0000	-12.48	-11.68	-.0014	-266.	-232.	5.698	-2.0	.0013	.197
		4.1	.000	.0	.0	.0000	.0	.0	-.0062	0.	0.	.0	.001	.0008	4.579
S971020	1.981	.6	.516	6.40	8.30	-.0110	-10.53	-10.63	-.0283	-381.	-160.	5.343	-1.8	.0012	.138
		1.8	.000	.0	.0	.0008	.0	.0	.0156	5.	13.	.0	.000	.0005	6.050
S000452	2.117	1.4	.507	6.40	8.30	-.0060	-9.74	-9.65	.0040	-191.	-251.	5.131	-1.7	.0009	.146
		3.9	.000	.0	.0	.0326	.0	.0	-.0459	0.	0.	.0	.001	.0006	2.957
S980257	2.291	1.3	.490	6.26	8.23	-.0036	-8.51	-8.30	-.0122	-286.	-245.	4.925	-1.6	.0013	.166
		3.1	.000	.0	.0	.0137	.0	.0	-.0099	5.	5.	.0	.002	.0006	5.463
S000560	3.230	.3	.399	5.10	7.60	.0070	-4.77	-6.00	.0232	-200.	-200.	3.652	-6.0	.0020	.190
		.8	.000	.0	.0	.0111	.0	.0	.0199	0.	0.	.0	-.009	.0007	7.893
S000561	3.324	.6	.403	4.37	7.07	.0000	-4.24	-5.20	.0179	-200.	-200.	3.647	-6.0	.0015	.208
		1.8	.000	.0	.0	.0000	.0	.0	.0109	0.	0.	.0	-.007	.0007	5.042
S000557	3.542	.7	.390	5.63	7.91	.0000	-4.38	-4.41	.0052	-200.	-200.	3.522	-6.0	.0019	.210
		2.2	.000	.0	.0	.0000	.0	.0	.0198	0.	0.	.0	.002	.0005	4.631

Table D-12: 0.8 Elliptical 6DOF Aerodynamics – Multiple Fits

Shot Numbers		Mach Number	DBSQ ABARM	CX CXa2 CXB2	CYB CYB3 CYga3	CZA CZa2 CZa3	CnB CnB3 Cnga3	Cma Cma2 Cma3	Cnr Cnr2 Cmga3	Cmq Cmq2	CXaB2 CNaB3 CmaB3	Clp Clga2	Standard Error X(m) Y-Z(m)	Standard Error Angle(deg) Roll(deg)
S980927	S980926	.638	3.2	.288	7.82	10.18	-15.68	-15.19	142.	-456.	3.000	-5.54	.0017	.285
			2.8	.00	.0	.0	.0	.0	0.	0.	.0	.00	.0007	4.875
				.00	.0	.0	.0	.0	.0		.0			
S980940	S980259	1.330	1.2	.596	8.11	10.43	-14.91	-16.12	-231.	-216.	.500	-4.50	.0018	.203
S980942			3.2	.00	.0	.0	.0	.0	0.	0.	.0	.00	.0006	4.826
				.00	.0	.0	.0	.0	.0		.0			
S971020	S980257	2.136	1.0	.506	6.38	8.25	-9.54	-9.43	-334.	-209.	-9.042	-3.86	.0014	.158
			3.0	.00	.0	.0	.0	.0	6.	7.	.0	.00	.0006	5.616
				.00	.0	.0	.0	.0	.0		.0			
S000561	S000557	3.433	.7	.396	5.07	7.60	-4.34	-4.95	-100.	-211.	3.522	-6.00	.0018	.200
			2.2	.00	.0	.0	.0	.0	0.	3.	.0	.00	.0006	4.786
				.00	.0	.0	.0	.0	.0		.0			

4. 0.6 Elliptical

Table D-13: 0.6 Elliptical Model Physical Properties

Shot Number	Projectile Diameter (mm)	Mass (kg)	Axial Inertia (kg- m2)	Inertia Y (kg- m2)	Inertia Z (kg- m2)	Inertia XY (kg- m2)	Length (mm)	CG (mm from nose)	Spin
S980929	17.000	.916E-01	.426E-05	.129E-03	.127E-03	.000	137.500	64.831	Yes
S980945	17.000	.916E-01	.423E-05	.129E-03	.127E-03	.000	137.500	64.802	Yes
S980932	17.000	.920E-01	.426E-05	.130E-03	.128E-03	.000	137.500	64.742	Yes
S980933	17.000	.918E-01	.423E-05	.129E-03	.127E-03	.000	137.500	64.883	Yes
S980936	17.000	.916E-01	.423E-05	.129E-03	.127E-03	.000	137.500	64.802	Yes
S980937	17.000	.916E-01	.423E-05	.129E-03	.127E-03	.000	137.500	64.802	Yes
S980939	17.000	.916E-01	.423E-05	.129E-03	.127E-03	.000	137.500	64.802	Yes
S980943	17.000	.916E-01	.423E-05	.129E-03	.127E-03	.000	137.500	64.802	Yes
S980941	17.000	.916E-01	.423E-05	.129E-03	.127E-03	.000	137.500	64.802	Yes
S000447	17.000	.916E-01	.423E-05	.129E-03	.127E-03	.000	137.500	64.802	Yes
S991181	17.000	.916E-01	.423E-05	.129E-03	.127E-03	.000	137.500	64.883	Yes
S990526	17.000	.916E-01	.423E-05	.129E-03	.127E-03	.000	137.500	64.802	Yes
S000446	17.000	.916E-01	.423E-05	.129E-03	.127E-03	.000	137.500	64.803	Yes
S000556	17.000	.916E-01	.423E-05	.129E-03	.127E-03	.000	137.500	64.802	Yes

Table D-14: 0.6 Elliptical Range Conditions

Shot Number	No. of Stations	Observed Distance (m)	Pressure (mbar)	Temperature (degrees C)	Relative Humidity %	Air Density (kg/m3)	Speed of Sound (m/sec)	Reynolds Number (x10**-7)
S980929	25	80.8	1014.90000	21.67	58.0000	1.1992	344.210	.209
S980945	27	100.6	1013.89000	21.16	56.0000	1.2001	343.912	.235
S980932	29	100.6	1018.63000	21.11	57.0000	1.2059	343.883	.251
S980933	28	105.2	1015.92000	20.97	57.0000	1.2033	343.801	.299
S980936	29	105.2	1016.26000	20.90	54.0000	1.2040	343.760	.340
S980937	31	105.2	1017.27000	21.46	56.0000	1.2029	344.087	.347
S980939	44	199.7	1016.26000	20.97	54.0000	1.2037	343.801	.412
S980943	42	198.1	1015.92000	20.28	54.0000	1.2061	343.398	.433
S980941	41	169.3	1016.26000	20.97	54.0000	1.2037	343.801	.433
S000447	26	100.6	1021.68000	20.07	55.0000	1.2138	343.275	.757
S991181	20	82.2	1021.00000	19.10	54.0000	1.2171	342.706	.853
S990526	45	199.7	1021.34000	20.62	57.0000	1.2112	343.597	.973
S000446	46	199.6	1021.68000	20.07	55.0000	1.2138	343.275	1.043
S000556	44	190.4	1021.34000	19.31	58.0000	1.2166	342.830	1.047

Table D-15: 0.6 Elliptical 6DOF Aerodynamics – Single Fits

Shot Number	Mach Number	DBSQ ABARM	CX CXA2	CYB CYB3	CZA CZA2	CY0 CZ0	CnB CnB3	Cma Cma3	Cn0 Cm0	Cnr Cnr2	Cmq Cmq2	CXaB2 CmaB3	Clp Cld	Standard Error X(m) Y-Z(m)	Angle(deg) Roll(deg)
S980929	.670	.3	.309	7.49	10.93	.0136	-12.00	-12.79	.0268	-120.	-200.	******	-20.0	.0020	.145
		1.1	.000	.0	.0	.0325	.0	.0	-.0287	0.	0.	-400.0	.006	.0006	2.359
S980945	.754	5.5	.330	8.44	12.72	-.0336	-12.41	-12.84	-.0660	-61.	-261.	-8.271	-19.0	.0015	.194
		6.0	.000	.0	.0	-.0113	.0	.0	.0268	0.	0.	-405.5	-.003	.0008	5.735
S980932	.801	1.9	.353	7.00	12.21	.0130	-12.18	-13.34	.0306	-178.	-244.	******	-22.5	.0014	.218
		4.1	.000	.0	.0	.0287	.0	.0	-.0361	0.	0.	-423.9	-.014	.0006	3.115
S980933	.957	5.9	.387	7.00	19.49	.0232	-14.20	-22.51	.0519	-100.	-259.	1.500	-2.1	.0018	.290
		8.7	.000	.0	.0	-.0084	.0	.0	.0028	71.	-243.	.0	.001	.0006	4.673
S980936	1.086	7.9	.613	8.50	15.69	.0000	-17.17	-18.78	.0280	-200.	-250.	1.500	-2.3	.0011	.289
		7.3	.000	.0	.0	.0000	.0	.0	-.2264	0.	0.	.0	-.015	.0007	6.256
S980937	1.112	.7	.610	7.00	15.00	.0000	-14.10	-20.70	-.0024	-168.	-283.	1.500	-2.3	.0018	.185
		1.8	.000	.0	.0	.0000	.0	.0	.0168	8.	90.	.0	.002	.0005	2.494
S980939	1.316	1.0	.615	11.50	14.17	.0304	-12.47	-13.59	.0421	-96.	-261.	******	-25.7	.0016	.175
		3.1	.000	.0	.0	.0104	.0	.0	-.0283	0.	0.	.0	.001	.0008	7.242
S980943	1.382	.8	.601	11.50	15.00	.0556	-12.17	-13.63	.0696	-150.	-205.	******	-9.6	.0015	.232
		2.5	.000	.0	.0	.0697	.0	.0	-.0756	0.	0.	.0	.003	.0007	4.481
S980941	1.383	.9	.613	11.50	14.50	.0153	-12.93	-13.12	.0194	-125.	-268.	******	-9.3	.0019	.182
		2.4	.000	.0	.0	.0405	.0	.0	-.0272	0.	0.	.0	.008	.0005	4.732
S000447	2.397	4.9	.490	5.80	9.56	.0000	-6.99	-6.59	-.0054	-42.	-292.	4.670	-1.0	.0011	.178
		5.7	.000	.0	.0	.0000	.0	.0	-.0267	0.	0.	.0	-.004	.0007	8.187
S991181	2.694	4.4	.447	5.50	9.00	.0031	-5.74	-4.94	.0018	-200.	-324.	4.294	-2.0	.0037	.150
		3.4	.000	.0	.0	.0760	.0	.0	-.1594	0.	0.	.0	-.003	.0006	3.331
S990526	3.092	.9	.422	3.92	8.10	.0000	-4.09	-3.66	.0209	-92.	-214.	3.736	-8.0	.0017	.206
		1.7	.000	.0	.0	.0000	.0	.0	-.0212	0.	0.	.0	.014	.0012	6.297
S000446	3.306	.5	.406	4.50	8.00	.0000	-3.92	-3.24	-.0049	-72.	-161.	3.653	-1.1	.0015	.212
		1.6	.000	.0	.0	.0000	.0	.0	-.0071	0.	0.	.0	.000	.0010	.000
S000556	3.451	4.1	.400	4.02	8.45	-.0093	-4.16	-2.96	-.0069	-151.	-220.	3.518	-1.0	.0021	.285
		6.1	.000	.0	.0	-.0025	501.7	-156.7	.0427	0.	0.	.0	-.003	.0016	.000

Table D-16: 0.6 Elliptical 6DOF Aerodynamics – Multiple Fits

Shot Numbers		Mach Number	DBSQ ABARM	CX CXa2 CXB2	CYB CYB3 CYga3	CZA CZa2 CZa3	CnB CnB3 Cnga3	Cma Cma2 Cma3	Cnr Cnr2 Cmga3	Cmq Cmq2	CXaB2 CNaB3 CmaB3	Clp Clga2	Standard Error X(m) Y-Z(m)	Angle(deg) Roll(deg)
S980932	S980929	.742	2.6	.332	7.45	11.81	-12.46	-12.99	-86.	-274.	******	-19.66	.0018	.204
S980945			6.0	.00	.0	.0	.0	.0	0.	0.	0.0	.00	.0007	4.006
				.00	.0	.0	.0	.0	.0		-391.5			
S980937	S980936	1.099	4.5	.610	7.11	15.02	-14.76	-18.84	-179.	-303.	2.000	-3.64	.0016	.166
			7.9	.00	.0	.0	.0	.0	28.	41.	.0	.00	.0006	4.669
				.00	.0	.0	.0	.0	.0		-265.4			
S980939	S980943	1.360	1.0	.614	11.90	14.81	-12.59	-13.72	-184.	-201.	******	-12.18	.0018	.260
S980941			2.9	.00	.0	.0	.0	.0	0.	0.	.0	17.95	.0006	4.773
				.00	.0	.0	.0	.0	.0		.0			
S000447	S991181	2.547	4.6	.466	5.79	9.43	-6.27	-5.66	-50.	-311.	4.294	1.57	.0025	.167
			5.7	.00	.0	.0	-110.0	.0	4.	5.	.0	.00	.0012	5.025
				.00	.0	.0	.0	-109.2	.0		.0			
S000446	S000556	3.379	2.5	.402	4.53	8.30	-3.95	-3.03	-111.	-192.	3.518	-.98	.0021	.291
			5.9	.00	.0	.0	17.5	.0	1.	1.	.0	.00	.0014	.000
				.00	.0	.0	.0	-166.9	.0		.0			

5. Blended Elliptical

Table D-17: Blended Elliptical Model Physical Properties

Shot Number	Projectile Diameter (mm)	Mass (kg)	Axial Inertia (kg- m2)	Inertia Y (kg- m2)	Inertia Z (kg- m2)	Inertia XY (kg- m2)	Length (mm)	CG (mm from nose)	Spin
S981157	17.000	.910E-01	.399E-05	.141E-03	.140E-03	.000	137.500	63.304	Yes
S981155	17.000	.910E-01	.396E-05	.142E-03	.140E-03	.000	137.500	63.402	Yes
S981159	17.000	.914E-01	.403E-05	.142E-03	.141E-03	.000	137.500	63.513	Yes
S981161	17.000	.908E-01	.396E-05	.141E-03	.140E-03	.000	137.500	63.542	Yes
S981162	17.000	.908E-01	.396E-05	.142E-03	.140E-03	.000	137.500	63.639	Yes
S990166	17.000	.909E-01	.396E-05	.141E-03	.140E-03	.000	137.500	63.604	Yes
S990169	17.000	.908E-01	.396E-05	.142E-03	.140E-03	.000	137.500	63.441	Yes
S990168	17.000	.908E-01	.396E-05	.141E-03	.140E-03	.000	137.500	63.674	Yes
S990167	17.000	.916E-01	.403E-05	.142E-03	.141E-03	.000	137.500	63.694	Yes
S991285	17.000	.910E-01	.398E-05	.141E-03	.141E-03	.000	137.500	63.547	Yes
S991284	17.000	.912E-01	.401E-05	.142E-03	.142E-03	.000	137.500	63.653	Yes

Table D-18: Blended Elliptical Range Conditions

Shot Number	No. of Stations	Observed Distance (m)	Pressure (mbar)	Temperature (degrees C)	Relative Humidity %	Air Density (kg/m3)	Speed of Sound (m/sec)	Reynolds Number (x10**-7)
S981157	20	71.6	1014.23000	19.72	58.0000	1.2064	343.070	.195
S981155	24	82.3	1014.23000	20.21	58.0000	1.2044	343.357	.199
S981159	21	74.7	1014.56000	20.00	55.0000	1.2057	343.234	.203
S981161	30	123.4	1017.95000	19.23	60.0000	1.2129	342.783	.304
S981162	32	128.0	1015.92000	20.34	60.0000	1.2059	343.433	.305
S990166	29	100.6	1014.23000	20.00	58.0000	1.2053	343.234	.316
S990169	38	169.2	1028.45000	19.44	69.0000	1.2245	342.906	.444
S990168	43	179.8	1028.45000	19.44	69.0000	1.2245	342.906	.477
S990167	36	146.4	1014.23000	20.00	58.0000	1.2053	343.234	.472
S991285	11	39.6	1016.60000	21.94	45.0000	1.2001	344.368	.805
S991284	10	36.6	1031.16000	21.18	43.0000	1.2205	343.924	.832

Table D-19: Blended Elliptical 6DOF Aerodynamics – Single Fits

Shot Number	Mach Number	DBSQ ABARM	CX CXA2	CYB CYB3	CZA CZA2	CY0 CZ0	CnB CnB3	Cma Cma3	Cn0 Cm0	Cnr Cnr2	Cmq Cmq2	CXaB2 CmaB3	Clp Cld	Standard Error X(m) Y-Z(m)	Standard Error Angle(deg) Roll(deg)
S981157	.623	3.6	.298	7.39	9.00	.0320	-14.83	-14.66	.0745	118.	-516.	3.354	-1.9	.0009	.171
		2.9	.000	.0	.0	.0274	.0	.0	-.0248	0.	0.	.0	.001	.0005	3.299
S981155	.636	1.9	.299	6.73	9.00	.0202	-15.24	-15.01	.0611	375.	-268.	3.386	-1.9	.0011	.208
		2.3	.000	.0	.0	-.0057	.0	.0	.0463	0.	0.	.0	-.002	.0005	4.813
S981159	.649	2.8	.294	7.49	9.89	.0344	-15.39	-14.25	.0791	192.	-200.	3.417	-1.9	.0010	.179
		2.5	.000	.0	.0	.0333	.0	.0	-.0091	0.	0.	.0	-.001	.0004	2.792
S981161	.964	1.0	.380	8.62	11.68	-.0172	-19.24	-25.27	-.0352	-60.	-301.	4.742	-2.1	.0011	.201
		2.4	.000	.0	.0	.0029	.0	.0	.0523	0.	0.	.0	-.001	.0003	2.221
S981162	.972	1.1	.417	8.12	16.13	-.0021	-19.14	-24.30	.0031	-123.	-266.	4.859	-2.1	.0011	.136
		2.2	.000	.0	.0	-.0348	.0	.0	.0974	0.	0.	.0	.001	.0004	3.460
S990166	1.007	1.3	.528	9.81	12.34	-.0206	-18.31	-24.53	-.0457	-203.	-268.	5.354	-2.2	.0020	.149
		2.8	.000	.0	.0	.0648	.0	.0	-.0716	0.	0.	.0	.000	.0004	3.334
S990169	1.395	1.3	.598	8.50	13.00	-.0014	-14.80	-15.98	.0027	-230.	-310.	7.046	-2.2	.0013	.147
		2.7	.000	.0	.0	-.0589	.0	.0	.1655	6.	9.	.0	-.001	.0004	3.158
S990168	1.497	2.4	.579	8.00	12.73	-.0035	-14.87	-15.76	-.0184	-181.	-275.	6.716	-2.2	.0011	.125
		3.9	.000	.0	.0	-.0517	.0	.0	.1476	0.	0.	.0	-.001	.0005	4.726
S990167	1.504	.4	.598	9.00	13.00	.0000	-15.30	-15.14	.0047	-172.	-222.	6.577	-2.1	.0014	.228
		1.2	.000	.0	.0	.0000	.0	.0	.0827	10.	10.	.0	.002	.0005	2.695
S991285	2.584	5.7	.465	6.15	8.35	-.0201	-6.29	-6.88	-.0281	-35.	-319.	4.406	-1.3	.0008	.159
		4.5	.000	.0	.0	-.0334	.0	.0	.2321	0.	0.	.0	-.001	.0006	1.882
S991284	2.623	9.3	.454	4.35	8.82	.0140	-7.91	-6.76	.0674	-80.	-219.	4.348	-1.3	.0006	.113
		5.3	.000	.0	.0	-.0192	.0	.0	.2440	0.	0.	.0	-.002	.0004	4.573

Table D-20: Blended Elliptical 6DOF Aerodynamics – Multiple Fits

Shot Numbers		Mach Number	DBSQ ABARM	CX CXa2 CXB2	CYB CYB3 CYga3	CZA CZa2 CZa3	CnB CnB3 Cnga3	Cma Cma2 Cma3	Cnr Cnr2 Cmga3	Cmq Cmq2	CXaB2 CNaB3 CmaB3	Clp Clga2	Standard Error X(m) Y-Z(m)	Standard Error Angle(deg) Roll(deg)
S981157	S981155	.636	2.6	.298	6.55	9.75	-15.08	-14.48	185.	-268.	3.417	-1.93	.0011	.259
S981159			3.1	.00	.0	.0	.0	.0	0.	0.	.0	.00	.0005	3.689
				.00	.0	.0	.0	.0	.0		.0			
S990166	S981162	.982	1.1	.448	8.00	13.00	-19.06	-24.66	-100.	-268.	4.742	-2.14	.0039	.213
S981161			2.7	.00	.0	.0	.0	.0	0.	0.	.0	.00	.0004	3.045
				.00	.0	.0	.0	.0	.0		.0			
S990167	S990168	1.466	1.1	.594	10.00	13.00	-14.47	-15.86	-176.	-353.	7.046	-2.20	.0030	.292
S990169			3.0	.00	.0	.0	.0	.0	5.	8.	.0	-5.14	.0005	3.481
				.00	.0	.0	.0	.0	.0		.0			
S991285	S991284	2.604	7.4	.460	4.53	8.71	-7.74	-6.84	-25.	-270.	4.348	-1.32	.0008	.152
			5.3	.00	.0	.0	.0	.0	0.	0.	.0	.00	.0005	3.367
				.00	.0	.0	.0	.0	.0		.0			

6. Square

Table D-21: Square Model Physical Properties

Shot Number	Projectile Diameter (mm)	Mass (kg)	Axial Inertia (kg- m2)	Inertia Y (kg- m2)	Inertia Z (kg- m2)	Inertia XY (kg- m2)	Length (mm)	CG (mm from nose)	Spin
S000214	17.000	.853E-01	.384E-05	.130E-03	.130E-03	.000	137.396	59.520	Yes
S991069	17.000	.853E-01	.383E-05	.130E-03	.130E-03	.000	137.396	59.593	Yes
S991068	17.000	.851E-01	.384E-05	.131E-03	.131E-03	.000	137.396	59.775	Yes
S000215	17.000	.853E-01	.384E-05	.130E-03	.130E-03	.000	137.396	59.520	Yes
S991077	17.000	.850E-01	.380E-05	.129E-03	.129E-03	.000	137.396	59.538	Yes
S991076	17.000	.850E-01	.380E-05	.129E-03	.129E-03	.000	137.396	59.538	Yes
S000454	17.000	.853E-01	.384E-05	.130E-03	.130E-03	.000	137.396	59.520	Yes
S991072	17.000	.850E-01	.384E-05	.130E-03	.130E-03	.000	137.396	59.593	Yes
S991180	17.000	.854E-01	.384E-05	.131E-03	.131E-03	.000	137.396	59.259	Yes
S000450	17.000	.853E-01	.384E-05	.130E-03	.130E-03	.000	137.396	59.520	Yes
S000448	17.000	.853E-01	.384E-05	.130E-03	.130E-03	.000	137.396	59.520	Yes
S000455	17.000	.853E-01	.384E-05	.130E-03	.130E-03	.000	137.396	59.520	Yes
S000564	17.000	.853E-01	.384E-05	.130E-03	.130E-03	.000	137.396	59.520	Yes

Table D-22: Square Range Conditions

Shot Number	No. of Stations	Observed Distance (m)	Pressure (mbar)	Temperature (degrees C)	Relative Humidity %	Air Density (kg/m3)	Speed of Sound (m/sec)	Reynolds Number (x10**-7)
S000214	19	71.6	1014.90000	18.33	57.0000	1.2130	342.255	***
S991069	30	128.0	1017.95000	20.42	56.0000	1.2080	343.480	.266
S991068	33	137.2	1017.95000	20.42	56.0000	1.2080	343.480	.269
S000215	31	128.0	1024.72000	18.61	54.0000	1.2235	342.419	.386
S991077	46	199.7	1025.06000	19.79	52.0000	1.2190	343.111	.428
S991076	48	199.6	1025.40000	19.86	52.0000	1.2191	343.152	.463
S000454	44	198.1	1014.23000	19.51	59.0000	1.2073	342.947	.584
S991072	44	198.1	1026.76000	20.56	49.0000	1.2178	343.561	.693
S991180	44	195.2	1024.72000	20.00	53.0000	1.2177	343.234	.800
S000450	49	199.7	1019.30000	19.38	59.0000	1.2139	342.871	.822
S000448	43	195.2	1019.30000	19.38	59.0000	1.2139	342.871	.824
S000455	47	199.6	1014.23000	19.51	59.0000	1.2073	342.947	1.015
S000564	47	199.6	1018.63000	20.07	61.0000	1.2102	343.275	1.073

Table D-23: Square 6DOF Aerodynamics – Single Fits

Shot Number	Mach Number	DBSQ ABARM	CX CX2	CNa CNa3	CYpa Cnpa	Cma Cma3	Cmq Cmq2	CZga3 Cmga3	CYga3 Cnga3	Clga2 Cnsm	Clp Cld	CNda CNdB	Cmda CmdB	Standard Error X(m) Y-Z(m)	Standard Error Angle(deg) Roll(deg)
S000214	.553	2.3	.332	7.69	.00	-18.679	-297.4	.0	.0	.00	-1.890	.003	.033	.0014	.271
		2.0	3.30	.0	.0	.0	.0	.0	.0	-1.55	.003	-.021	-.074	.0007	3.002
S991069	.849	.2	.356	7.61	.00	-19.663	-241.9	.0	.0	.00	-6.000	.008	-.024	.0005	.233
		.8	3.97	.0	.0	.0	.0	.0	.0	-1.89	.007	-.001	.001	.0008	2.261
S991068	.858	.1	.348	9.11	.00	-20.826	-322.5	.0	.0	.00	-6.000	.000	.005	.0005	.185
		.9	3.98	.0	.0	.0	.0	.0	.0	.00	.000	.000	-.009	.0005	2.159
S000215	1.211	.3	.613	9.16	.00	-20.771	-350.8	.0	.0	.00	-6.000	.000	-.008	.0005	.137
		1.8	7.62	.0	.0	.0	.0	.0	.0	.00	.003	.000	-.005	.0003	5.808
S991077	1.351	.6	.606	11.92	.00	-19.887	-280.2	.0	.0	.00	-6.000	.000	.001	.0006	.141
		2.3	7.41	.0	.0	.0	.0	.0	.0	.00	.005	.000	-.002	.0002	4.217
S991076	1.462	.6	.597	9.17	.00	-19.733	-314.4	.0	.0	.00	-6.000	.002	-.016	.0006	.121
		2.5	6.92	.0	.0	.0	.0	.0	.0	.00	.009	.001	.010	.0006	6.108
S000454	1.862	.5	.565	10.90	.00	-16.383	-262.3	.0	.0	.00	-6.000	-.012	.028	.0007	.085
		2.2	5.75	.0	.0	.0	.0	.0	.0	.00	.008	.007	.024	.0004	6.950
S991072	2.190	.2	.528	8.32	.00	-11.717	-302.0	.0	.0	.00	-6.000	.000	.011	.0006	.121
		1.5	5.05	.0	.0	.0	.0	.0	.0	.00	-.003	.000	-.013	.0006	6.839
S991180	2.527	1.2	.493	8.05	.00	-9.783	-224.7	.0	.0	.00	-6.000	.000	.015	.0008	.162
		2.9	4.64	.0	.0	.0	.0	.0	.0	.00	.005	.000	.012	.0005	6.001
S000450	2.606	.2	.483	7.50	.00	-8.906	-215.6	.0	.0	.00	-6.000	.000	.010	.0008	.121
		1.3	4.43	.0	.0	.0	.0	.0	.0	.00	.010	.000	.024	.0004	8.066
S000448	2.612	1.7	.477	7.49	.00	-9.772	-217.2	.0	.0	.00	-6.000	-.001	.025	.0006	.105
		3.9	4.49	.0	.0	.0	.0	.0	.0	.00	-.003	.010	.029	.0006	4.405
S000455	3.233	.9	.431	7.08	.00	-7.040	-154.9	.0	.0	.00	-6.000	-.035	.098	.0008	.152
		1.7	3.67	.0	.0	.0	.0	.0	.0	.00	-.002	.014	.047	.0006	8.919
S000564	3.411	.3	.421	6.62	.00	-6.276	-163.9	.0	.0	.00	-5.813	.000	.011	.0007	.116
		1.0	3.60	.0	.0	.0	.0	.0	.0	.00	-.024	.000	.002	.0005	10.250

Table D-24: Square 6DOF Aerodynamics – Multiple Fits

Shot Numbers		Mach Number	DBSQ ABARM	CX CX2 CX4	CNa CNa3 CNa5	CYpa Cnpa Cnpa3	Cma Cma3 Cma5	Cmq Cmq2 Cmq4	CZga3 Cmga3 Cmga	CYga3 Cnga3 Cnga5	Clga2 CXga2 Clp	CXM CmaM CnsM	Standard Error X(m) Y-Z(m)	Standard Error Angle(deg) Roll(deg)
S991068	S991069	.853	.2	.354	8.00	.00	-19.817	-209.3	.0	.0	.00	-.09	.0005	.221
			.9	3.97	.0	.00	.0	.0	.0	.0	.00	.00	.0007	2.186
				.0	.0	.0	.0	.0	.0	.0	-6.00	-1.43		
S000215	S991077	1.337	.5	.605	10.27	.00	-20.230	-308.9	.0	.0	.00	-.16	.0006	.130
S991076			2.5	6.92	.0	.00	.0	.0	.0	.0	.00	3.30	.0004	5.275
				.0	.0	.0	.0	.0	.0	.0	-6.00	.00		
S000454	S991072	2.026	.4	.549	9.53	.00	-14.273	-280.4	.0	.0	.00	-.11	.0006	.097
			2.2	5.05	.0	.00	.0	.0	.0	.0	.00	12.07	.0005	6.810
				.0	.0	.0	.0	.0	.0	.0	-6.00	.00		
S991072	S991180	2.484	.8	.496	7.44	.00	-10.402	-224.8	.0	.0	.00	-.10	.0009	.131
S000450	S000448		3.9	4.49	.0	.00	.0	.0	.0	.0	.01	4.62	.0005	6.747
				.0	.0	.0	.0	.0	.0	.0	-4.00	.00		
S000455	S000564	3.323	.6	.425	7.01	.00	-6.869	-158.6	.0	.0	.00	-.08	.0008	.135
			1.7	3.60	.0	.00	.0	.0	.0	.0	.00	4.21	.0006	9.436
				.0	.0	.0	.0	.0	.0	.0	-5.87	.00		

7. Triangular

Table D-25: Triangular Model Physical Properties

Shot Number	Projectile Diameter (mm)	Mass (kg)	Axial Inertia (kg- m2)	Inertia Y (kg- m2)	Inertia Z (kg- m2)	Inertia XY (kg- m2)	Length (mm)	CG (mm from nose)	Spin
R000213	17.000	.824E-01	.405E-05	.123E-03	.123E-03	.000	137.396	59.549	Yes
S000211	17.000	.818E-01	.404E-05	.123E-03	.123E-03	.000	137.396	59.527	Yes
S000217	17.000	.824E-01	.405E-05	.123E-03	.123E-03	.000	137.396	59.549	Yes
S000212	17.000	.824E-01	.405E-05	.123E-03	.123E-03	.000	137.396	59.527	Yes
S000220	17.000	.824E-01	.405E-05	.123E-03	.123E-03	.000	137.396	59.549	Yes
S000216	17.000	.824E-01	.405E-05	.123E-03	.123E-03	.000	137.396	59.549	Yes
S000221	17.000	.824E-01	.405E-05	.123E-03	.123E-03	.000	137.396	59.549	Yes
S991075	17.000	.823E-01	.404E-05	.123E-03	.123E-03	.000	137.396	59.597	Yes
S000210	17.000	.818E-01	.404E-05	.123E-03	.123E-03	.000	137.396	59.527	Yes
S991078	17.000	.823E-01	.404E-05	.123E-03	.123E-03	.000	137.396	59.626	Yes
S991074	17.000	.826E-01	.404E-05	.123E-03	.123E-03	.000	137.396	59.410	Yes
S991070	17.000	.827E-01	.407E-05	.124E-03	.124E-03	.000	137.396	59.782	Yes
S000451	17.000	.824E-01	.405E-05	.123E-03	.123E-03	.000	137.396	59.549	Yes
S991071	17.000	.827E-01	.407E-05	.123E-03	.123E-03	.000	137.396	59.352	Yes
S991079	17.000	.818E-01	.404E-05	.123E-03	.123E-03	.000	137.396	59.527	Yes
S000562	17.000	.824E-01	.405E-05	.123E-03	.123E-03	.000	137.396	59.549	Yes
S000563	17.000	.824E-01	.505E-05	.123E-03	.123E-03	.000	137.396	59.549	Yes
S000565	17.000	.824E-01	.405E-05	.123E-03	.123E-03	.000	137.396	59.549	Yes

Table D-26: Triangular Range Conditions

Shot Number	No. of Stations	Observed Distance (m)	Pressure (mbar)	Temperature (degrees C)	Relative Humidity %	Air Density (kg/m3)	Speed of Sound (m/sec)	Reynolds Number (x10**-7)
R000213	18	71.6	1014.90000	18.33	57.0000	1.2130	342.255	***
S000211	25	80.8	1026.76000	18.27	50.0000	1.2274	342.219	.200
S000217	25	100.6	1026.08000	18.61	53.0000	1.2252	342.419	.281
S000212	29	105.2	1021.34000	18.54	49.0000	1.2198	342.378	.282
S000220	31	114.3	1026.08000	18.61	53.0000	1.2252	342.419	.290
S000216	31	128.0	1024.72000	18.61	54.0000	1.2235	342.419	.357
S000221	33	128.0	1024.38000	18.54	54.0000	1.2234	342.378	.361
S991075	47	199.7	1025.40000	19.86	52.0000	1.2191	343.152	.408
S000210	27	105.2	1026.76000	18.27	50.0000	1.2274	342.219	.429
S991078	45	199.6	1025.06000	19.79	52.0000	1.2190	343.111	.497
S991074	45	199.7	1025.40000	19.86	52.0000	1.2191	343.152	.508
S991070	50	199.6	1026.76000	20.42	48.0000	1.2184	343.480	.637
S000451	40	195.2	1018.63000	19.17	61.0000	1.2139	342.748	.729
S991071	36	181.4	1026.76000	20.56	49.0000	1.2178	343.561	.800
S991079	44	195.2	1024.72000	18.40	53.0000	1.2244	342.296	.836
S000562	42	199.6	1017.95000	19.93	60.0000	1.2100	343.193	1.044
S000563	45	199.6	1017.95000	19.93	60.0000	1.2100	343.193	1.054
S000565	40	195.2	1018.63000	20.07	61.0000	1.2102	343.275	1.059

Table D-27: Triangular 6DOF Aerodynamics – Single Fits

Shot Number	Mach Number	DBSQ ABARM	CX CX2	CNa CNa3	CYpa Cnpa	Cma Cma3	Cmq Cmq2	CZga3 Cmga3	CYga3 Cnga3	Clga2 Cnsm	Clp Cld	CNda CNdB	Cmda CmdB	Standard Error X(m) Y-Z(m)	Standard Error Angle(deg) Roll(deg)
R000213	.577	1.1	.304	7.83	.00	-15.042	-82.0	.0	.0	.00	-4.000	-.011	.015	.0009	.207
		1.7	3.30	.0	.0	.0	.0	.0	.0	.00	-.005	.023	.068	.0007	1.852
S000211	.624	1.6	.315	6.93	.00	-15.922	-20.1	.0	.0	.00	-4.669	.000	.000	.0007	.306
		2.2	3.36	.0	.0	.0	.0	.0	.0	.00	-.003	.000	.000	.0012	3.106
S000217	.883	5.6	.333	10.00	.00	-17.295	-271.9	.0	.0	.00	-8.000	.000	.016	.0010	.267
		7.0	-.23	.0	.0	-483.5	.0	.0	.0	.00	-.004	.000	-.009	.0014	4.477
S000212	.890	.2	.341	10.80	.00	-17.074	-300.0	.0	.0	.00	-8.000	.000	.005	.0006	.210
		1.0	4.15	.0	.0	.0	.0	.0	.0	.00	-.010	.000	-.001	.0012	3.557
S000220	.909	4.9	.354	10.87	.00	-17.991	-323.7	.0	.0	.00	-7.947	.000	-.004	.0010	.219
		7.3	-2.68	.0	.0	-446.4	.0	.0	.0	.00	-.016	.000	-.025	.0014	4.171
S000220	.909	4.9	.354	10.87	.00	-17.991	-323.7	.0	.0	.00	-7.947	.000	-.004	.0010	.219
		7.3	-2.68	.0	.0	-446.4	.0	.0	.0	.00	-.016	.000	-.025	.0014	4.171
S000221	1.134	2.3	.598	11.99	.00	-20.103	-276.5	.0	.0	.00	-2.305	-.007	.020	.0006	.280
		5.5	7.10	.0	.0	.0	.0	.0	.0	.00	.000	-.007	-.022	.0013	8.664
S991075	1.288	.3	.593	11.17	.00	-18.566	-300.0	.0	.0	.00	-2.319	-.047	.089	.0011	.199
		1.2	7.61	.0	.0	.0	.0	.0	.0	.00	-.001	-.017	-.027	.0011	4.157
S000210	1.344	.4	.583	9.00	.00	-17.236	-267.2	.0	.0	.00	-6.000	.000	-.012	.0009	.275
		2.1	7.11	.0	.0	.0	.0	.0	.0	.00	-.004	.000	.029	.0013	6.012
S991078	1.568	.4	.542	9.00	.00	-14.630	-244.4	.0	.0	.00	-2.133	-.018	.062	.0009	.296
		1.7	6.48	.0	.0	.0	.0	.0	.0	.00	.000	-.018	-.054	.0013	4.438
S991074	1.602	.4	.545	9.00	.00	-13.112	-342.8	.0	.0	.00	-2.127	.000	-.006	.0008	.222
		1.7	6.38	.0	.0	.0	.0	.0	.0	.00	.000	.000	.001	.0012	3.312
S991070	2.012	.2	.507	6.77	.00	-8.469	-299.9	.0	.0	.00	-1.735	.000	-.005	.0013	.267
		2.1	5.18	.0	.0	.0	.0	.0	.0	.00	-.001	.000	-.019	.0013	6.221
S000451	2.308	.4	.481	8.83	.00	-6.635	-228.3	.0	.0	.00	-1.515	.000	.000	.0013	.268
		2.4	4.79	.0	.0	.0	.0	.0	.0	.00	-.001	.000	.000	.0022	7.868
S991071	2.529	1.6	.465	6.47	.00	-6.056	-224.3	.0	.0	.00	-6.000	.000	.000	.0014	.234
		4.6	4.49	.0	.0	.0	.0	.0	.0	.00	-.010	.000	.000	.0017	5.839
S991079	2.625	.7	.457	9.70	.00	-5.915	-171.1	.0	.0	.00	-5.917	.017	-.018	.0012	.213
		2.9	4.35	.0	.0	.0	.0	.0	.0	.00	-.007	.020	.023	.0012	5.925
S000562	3.321	24.9	.366	6.11	.00	-4.178	-67.4	.0	.0	.00	-5.918	.000	.067	.0016	.432
		6.3	3.59	.0	.0	-91.6	.0	.0	.0	.00	-.015	.000	.044	.0018	5.330
S000563	3.352	1.6	.386	6.45	.00	-4.297	-177.2	.0	.0	.00	-3.503	.000	.016	.0011	.247
		2.3	3.58	.0	.0	.0	.0	.0	.0	.00	-.012	.000	-.036	.0014	4.971
S000565	3.369	.8	.386	6.78	.00	-4.125	-177.1	.0	.0	.00	-1.012	.000	-.012	.0009	.254
		2.6	3.57	.0	.0	.0	.0	.0	.0	.00	-.002	.000	-.008	.0013	6.581

Table D-28: Triangular 6DOF Aerodynamics – Multiple Fits

Shot Numbers		Mach	DBSQ	CX	CNa	CYpa	Cma	Cmq	CZga3	CYga3	Clga2	CXM	Standard Error X(m)	Standard Error Angle(deg)
		Number	ABARM	CX2	CNa3	Cnpa	Cma3	Cmq2	Cmga3	Cnga3	CXga2	CmaM	Y-Z(m)	Roll(deg)
				CX4	CNa5	Cnpa3	Cma5	Cmq4	Cmga	Cnga5	Clp	CnsM		
R000213	S000211	.601	1.4	.309	6.73	.00	-15.555	-33.1	.0	.0	.00	.21	.0011	.284
			2.3	3.36	.0	.00	.0	.0	.0	.0	-.20	-13.68	.0010	2.636
				.0	.0	.0	.0	.0	.0	.0	-4.59	.00		
S000212	S000217	.890	3.5	.344	10.38	.00	-17.554	-311.0	.0	.0	.00	.53	.0013	.235
S000220			7.2	-6.92	.0	.00	-431.5	.0	.0	.0	.04	-17.50	.0014	4.272
				.0	.0	.0	.0	.0	.0	.0	-8.57	.00		
S991075	S000221	1.181	1.4	.596	9.44	.00	-20.363	-297.7	.0	.0	.00	-.03	.0017	.266
S000216			5.1	6.99	.0	.00	.0	.0	.0	.0	.00	-2.34	.0012	6.285
				.0	.0	.0	.0	.0	.0	.0	-2.30	.00		
S991074	S991078	1.586	.4	.543	10.02	.00	-14.126	-273.9	.0	.0	.00	.00	.0019	.259
			1.6	6.48	.0	.00	.0	.0	.0	.0	-.02	18.64	.0013	3.907
				.0	.0	.0	.0	.0	.0	.0	-2.13	.00		
S000451	S991079	2.488	.8	.468	7.06	.00	-6.382	-210.0	.0	.0	.00	-.08	.0031	.251
S991071			4.5	4.49	.0	.00	.0	.0	.0	.0	.00	2.13	.0018	6.908
				.0	.0	.0	.0	.0	.0	.0	-6.00	.00		
S000565	S000563	3.360	1.1	.386	6.36	.00	-4.226	-173.9	.0	.0	.00	-.09	.0011	.258
			2.7	3.58	.0	.00	.0	.0	.0	.0	-.01	.00	.0014	5.923
				.0	.0	.0	.0	.0	.0	.0	-4.37	.00		

REFERENCES

1 Kittlye, R. L., Packard, J. D., Winchenbach, G. L., "Description and Capabilities of the Aeroballistic Research Facility", AFATL-TR-87-08, May 1987

2 Yates, L. A., "A Comprehensive Aerodynamic Data Reduction System For Aeroballistic Ranges", WL-TR-96-7059, October 1996

3 M.A. Fischer, and W.H. Hathaway, "ARFDAS Users Manual," AFATL-TR-88-48, Air Force Armament Laboratory, Eglin AFB, FL, November 1988

4 Murphy, C.H. , "Free Flight Motion of Symmetric Missiles", BRL Report 1216, Aberdeen Proving Ground, MD, July 1963

5 Murphy, C.H. , "Data Reduction for the Free Flight Spark Ranges", BRL Report 900, Aberdeen Proving Ground, MD, February 1954

6 Winchenbach, G. L., "Aerodynamic Testing In A Free-Flight Spark Range," WL-TR-1997-7006, Wright Laboratory, Armament Directorate, Weapon Flight Mechanics Division, Eglin AFB, FL, April 1997

7 Hathaway, W. H. and Whyte, R. H., "Aeroballistic Research Facility Free Flight Data Analysis Using The Maximum Likelihood Method," AFATL-TR-79-98, Air Force Armament Laboratory, Eglin AFB, FL, December 1979

INTENTIONALLY LEFT BLANK

DISTRIBUTION

AFRL-MN-EG-TR-2001-7082

Defense Technical Information Center
8725 John J. Kingman Road, Suite 0944
Fort Belvoir, VA 22060-6218 1

NASA Langley Research Center
Technical Library Branch, MS 185
Attn: Document Cataloging
Hampton, VA 23665 1

Commander
Naval Weapons Center (Code 3431)
Attn: Technical Library
China Lake, CA 93555-6001 1

Commander
U.S. Army Research Laboratory
Attn: AMSRL-OP-CI-B (Tech. Lib.)
Aberdeen Proving Ground, MD 21005 1

Director
U.S. Army Research Laboratory
Attn: Dr. Peter Plostins
Aberdeen Proving Ground, MD 21005 1

Director
U.S. Army Research Laboratory
Attn: F Brandon
Aberdeen Proving Ground, MD 21005 1

Director
U.S. Army Research Laboratory
Attn: Dr. Ed Schmidt
Aberdeen Proving Ground, MD 21005 1

Commander
U.S. Army Armament Research Development and
Engineering Center
Attn: SMCAR-TDC
Picatinny Arsenal, NJ 07806 1

Commander
U.S. Army Armament Research Development and
Engineering Center
Attn: AMSTA-AR-AET-A
Picatinny Arsenal, NJ 07806 1

Air University Library
600 Chennault Circle, Bldg 1405
Maxwell AFB, AL 36112-6424 1

Commander
U.S. Army Armament Research Development and
Engineering Center
Attn: AMSTA-AR-CCH-B
Picatinny Arsenal, NJ 07806 1

Commander
U.S. Army Armament Research Development and
Engineering Center
Attn: AMSTA-AR-FSE
Picatinny Arsenal, NJ 07806 1

Commander
U.S. Army Armament Research Development and
Engineering Center
Attn: AMSTA-AR-CCL-B
Picatinny Arsenal, NJ 07806 1

Commander
U.S. Army Armament Research Development and
Engineering Center
Attn: AMSTA-AR-CCH-A
Picatinny Arsenal, NJ 07806 1

Director
U.S. Army Research Office
PO Box 12211
Research Triangle Park, NC 27709-2211 1

Director
U.S. Army Benet Laboratory
Attn: SMCAR-CCB-R
Watervaliet, NY 12189 1

Director
U.S. Belvior Research Development and
Engineering Center
Attn: SATBE-FED
Ft. Belvior, VA 22060 1

Eglin AFB Offices:
AFRL/MN CA-N 1
AFRL/MNAV 10
AFRL / MNOC-1 (STINFO Office) 1

Arrow Tech Associates
1233 Shelburne Road, Suite D-8
South Burlington, Vermont 05403 2

Aeroprediction Incorporated
9449 Grover Drive, Suite 201
King George, VA 22485 2